SKIN FRICTION ON PILES AT THE NEW PUBLIC WORKS CENTRAL LABORATORY

GEO REPORT No. 38

J. Premchitt, I. Gray & K.K.S. Ho

First published, September 1994
First Reprint, April 1995

Prepared by:

Geotechnical Engineering Office,
Civil Engineering Department,
Civil Engineering Building,
101 Princess Margaret Road,
Homantin, Kowloon,
Hong Kong.

This publication is available from:

Government Publications Centre,
Ground Floor, Low Block,
Queensway Government Offices,
66 Queensway,
Hong Kong.

Overseas orders should be placed with:

Publications (Sales) Office,
Information Services Department,
28th Floor, Siu On Centre,
188 Lockhart Road, Wan Chai,
Hong Kong.

Price in Hong Kong: HK$97
Price overseas: US$16.5 (including surface postage)

An additional bank charge of **HK$50** or **US$6.50** is required per cheque made in currencies other than Hong Kong dollars.

Cheques, bank drafts or money orders
must be made payable to **HONG KONG GOVERNMENT**

PREFACE

In keeping with our policy of releasing information of general technical interest, we make available some of our internal reports in a series of publications termed the GEO Report series. The reports in this series, of which this is one, are selected from a wide range of reports produced by the staff of the Office and our consultants.

Copies of GEO Reports have previously been made available free of charge in limited numbers. The demand for the reports in this series has increased greatly, necessitating new arrangements for supply. In future a charge will be made to cover the cost of printing.

The Geotechnical Engineering Office also publishes guidance documents and presents the results of research work of general interest in GEO Publications. These publications and the GEO Reports are disseminated through the Government's Information Services Department. Information on how to purchase them is given on the last page of this report.

A. W. Malone
Principal Government Geotechnical Engineer
April 1995

EXPLANATORY NOTE

This GEO Report consists of two Special Project Reports on skin friction on piles at the new public works central laboratory.

They are presented in two separate sections in this Report. Their titles are as follows:

SECTION 1 : SKIN FRICTION ON PILES AT THE NEW PUBLIC WORKS CENTRAL LABORATORY

J. Premchitt & I. Gray

This report was originally produced in October 1987 as GCO Special Project Report No.SPR 2/87

FOREWORD

This report summarises the first part of a project to study the skin friction on driven precast concrete piles supporting the new Public Works Central Laboratory, which is being constructed on the Kowloon Bay reclamation under the supervision of the Architectural Services Department (Arch SD). The report describes the instrumentation of seven working piles, and presents the results obtained from monitoring the instruments during pile driving and load tests. These piles will continue to be monitored throughout construction and after completion of the building.

The project was initiated by G.E. Powell, J.M. Shen and K. Sivaloganathan of the Geotechnical Control Office Pile Study Group, and is being carried out in cooperation with Arch SD. W.K. Fung of Arch SD coordinated the instrumentation and piling. H. Kozuma of Daido Concrete (HK) Ltd., and Michael Chan of Franki Contractors Ltd. provided necessary assistance to the work. Those mentioned above, together with J.A. Williams of the Geotechnical Unit, Arch SD, provided a very helpful technical review of this report during drafting. These contributions are gratefully acknowledged.

J.B. Massey
Chief Geotechnical Engineer/Special Projects

CONTENTS

1. INTRODUCTION

Skin friction on the shaft of a pile is a major determining factor in the bearing capacity and settlement characteristics of the pile. It is dependent on the nature of the surrounding soil and the relative movement between the pile and the soil : downward movement of the soil causes 'negative' friction, while downward movement of the pile causes 'positive' friction. Realistic estimation of the magnitude of skin friction during construction and in the long term is very important in the analysis and design of pile foundations, especially in reclaimed land where ground settlement can induce negative skin friction and hence additional loads on the piles. However, very little relevant field data exist in Hong Kong, particularly for driven concrete piles.

The construction of the new four-storey Public Works Central Laboratory for the Materials Division, Geotechnical Control Office (GCO), on the Kowloon Bay reclamation, commenced in March 1987, under the supervision of the Architectural Services Department (Arch SD). The initial work included the driving of 172 number 500 mm diameter 'Daido' piles. The piles were prestressed, steam cured spun concrete, hollow in section. The foundation was designed by the successful tenderer, Franki Contractors Ltd. This foundation work provided an opportunity for long term field measurements of skin friction on working piles. Therefore, on the initiative of the GCO Pile Study Group and the Materials Division, the GCO recommended to Arch SD that instrumentation of these piles should be carried out to determine the mobilization of skin friction in the short and long term. The information to be obtained will help to ascertain the behaviour of the piles under actual loading conditions, verifying the design assumptions and demonstrating the functional adequacy of the piles.

The study commenced on 4 March. In order to comply with the construction schedule, all work related to instrumentation was completed in only 71 days, with the last instrumented pile being driven on 13 May. The scope of the present study was limited to the working piles, without other related investigations. Seven of the working piles were instrumented and five of these piles reached depths greater than 40 m. Load tests, up to 5400 kN, were carried out on three of the instrumented piles.

The instrumented piles were driven, and will be incorporated into the building, in exactly the same manner as the other working piles. Study of the behaviour of these working piles will provide a great advantage over other investigations conducted elsewhere on test piles under experimental conditions. However, instrument installation at the construction site, where the contractors were working to a tight schedule, posed many constraints, including little control over timing and a high risk of damage to the instruments.

This report (Part 1) summarises the instrumentation, and the results obtained from the initial monitoring, including monitoring during load testing of the piles. The load tests have provided detailed data on load distribution over the lengths of the piles. Good estimates of the mobilized skin friction and the division of load between skin friction and end bearing have been made from these data. They provide a basis for an initial assessment of the pile capacity and prediction of the pile performance in the long term.

These piles will be monitored throughout construction and after completion of the building. It is intended that a further report (Part 2) will be issued in about two years, when the results of long term monitoring are available. Another similar study is being initiated by the Geotechnical Unit, Arch SD and the Special Projects Division, GCO at the new Arch SD Depot building to be constructed on the To Kwa Wan reclamation, which will provide useful comparative data on the skin friction on piles.

In this report, a natural sign convention is used for strains, i.e. minus values indicate shortening (compression). However, where the term 'compressive strain' precedes a number, the negative sign is omitted.

2. PREVIOUS STUDIES

2.1 General

Skin friction on a pile can be readily determined from the distribution of axial force along the pile length (Broms, 1979 and Rieke & Crowser, 1987). The applied load and end bearing force act at the pile ends only. Therefore the difference in axial forces on any two sections of the pile is due solely to the skin friction acting on the pile surface between the two sections.

Figure 1 shows hypothetical distributions of axial force in a pile under various conditions. Figure 1(a) illustrates a case with no skin friction, resulting in uniform distribution of a constant axial force throughout the pile length. In this case, the end bearing force is equal to the applied load at the pile top. Figure 1(b) shows a case of uniform positive skin friction, in which axial force is decreasing with depth and there is no end bearing force.

In areas such as new reclamation sites, settlements can occur, and drag-down forces on piles can develop with time due to adhesion and friction between the soil strata and the pile surfaces (Broms, 1979; Lee & Lumb, 1982). In these cases negative skin friction is mobilized, causing higher axial forces with increasing depth, such as those illustrated in Figures 1(c) and 1(d). It is commonly observed that positive friction is also mobilized on the lower part of the pile in these cases, as shown in the two figures. Therefore, positive friction and end bearing force constitute the total pile resistance to the load imposed at the pile top plus the negative friction load. The separation point between the zone of negative friction and the zone of positive friction is the 'neutral point'. Its position may move under changing loading conditions (Okabe, 1977; Broms, 1979).

In practice, axial forces can normally be estimated, with good accuracy, from strains measured using strain gauges attached to, or embedded in, the pile. In most cases, the pile material can be assumed to be linearly elastic, and the pile has a uniform section. Therefore, strain and axial force can be directly related, and the strain and axial force distributions are identical in shape, differing only in scale.

Tomlinson (1977), Broms (1979) and Karlsrud & Haugen (1985) provide good reviews of available methods for calculating skin friction from engineering properties of soils. Some of the relevant formulae are given in Appendix C.2. Using these formulae, the results of field studies are commonly expressed in terms of adhesion factor α, related to undrained shear strength of soil, or friction factor β, related to effective overburden pressure.

2.2 Studies Elsewhere

Cooke (1981), of the Building Research Establishment (BRE), UK stated two main reasons for pile instrumentation. The first is to improve general design methods by investigating individual test piles over relatively short periods of time. These piles are generally not part of buildings. The second is to check the validity of the design methods employed for a particular building. This usually requires long term observation of working piles. There are few reported cases of the latter, due to the difficulty of maintaining regular observations for a long time, and the high instrument failure rate (Cooke, 1981).

The overseas studies reviewed are presented under these two categories below.

2.2.1 Test Piles

(a) Model piles. Tests on model piles are easier to conduct than those on full sized piles, but they suffer from the uncertainties of scale effects. Shibata (1982) studied negative friction on 60 mm diameter model piles in the laboratory. Other detailed studies, such as those by Cooke et al (1979), Karlsrud & Haugen (1985) and Konrad & Roy (1987) used jacked model piles (150 to 220 mm diameter), instead of driven piles, to prevent damage to the instruments. These were jacked into clay strata and then subjected to test loading. Typical results are shown in Figure 2(c), in which distributions of axial force under six test loads are given. Mobilized positive skin friction was sufficient to resist most of the load, and end bearing force was small.

(b) Bored piles. Instrumentation of large diameter bored piles can be carried out conveniently, with little risk of damage to instruments. Some previous studies are described by Mallard & Ballantyne (1976), Buttling (1976), Yong et al (1982), Costa Nunes et al (1985), Ting & Toh (1985) and Sharma et al (1986). Some results from Ting & Toh are presented in Figure 2(a) for a 1.2 m diameter, 43 m long bored pile in sandy soils, end-socketed in limestone, in Malaysia. The test load was fully taken up by positive skin friction. For a bored pile with a bell-shaped toe, some of the load could be carried in end bearing; a value of 60% was reported by Sharma et al for piles of this kind in Alberta oil sand deposits.

(c) Driven steel piles. This type of pile can be instrumented easily also, but driving stresses must be taken into account. Cases have been reported by Johannessen & Bjerrum (1965), Okabe (1977), Farid (1981), Fukuya et al (1982), Keenan & Bozozuk (1985) and Rieke & Crowser (1987). Results from Fukuya et al and Keenan & Bozozuk are presented in Figures 3(a) and 3(c) respectively. Fukuya et al used 610 mm diameter, 37.5 m long steel tube piles driven through sandy soils, in an area newly reclaimed from Tokyo Bay. Large negative friction developed in less than one year, corresponding to rapid ground settlement in the area. The average friction over the pile length was 36 kPa. Keenan & Bozozuk reported results for 320 mm diameter, 32 m long steel tube piles in silty soils in Canada. The development of positive friction on lower parts of the piles can be seen in both figures. These are similar to the hypothetical case (c) in Figure 1, where there is no working load.

(d) Driven concrete piles. Possibly due to the difficulties of instrumentation, there are few reported cases for this type of pile. Mallard & Ballantyne (1976) carried out tests on standard 'Raymond' step-tapered piles in corrugated steel shells, driven through fill and alluvium, and bearing on chalk. Concrete was placed in the shells by pumping after the shells were driven. The pile diameter was 440 m.m at the top, tapering to 240 mm at the toe, and the pile length was about 30 m. The results from a pile load test are shown in Figure 2(b). Rapid ground settlement occurred at the site and significant axial forces developed in the pile within a month, before the load test was carried out. The forces were caused by development of negative friction and they are also shown in the figure ('preload' force indicated on the left). Another reported case is by Mey et al (1985), who carried out tests on a 910 mm diameter, cylindrical prestressed Raymond pile.

2.2.2 Working Piles

There are relatively few cases of instrumentation of working piles with long term monitoring. Cooke (1981) reviewed four cases of instrumented piles actually supporting building loads. One of these cases was of driven piles. These studies were concerned with pile group effects and differences between interior and edge or corner piles. It was reported that peripheral piles usually take more load and have higher mobilized skin friction than interior piles.

Leung & Radhakhrisnan (1985) monitored the performance of working bored piles supporting a 42 storey building under construction in Singapore. The piles were formed in weathered siltstone. Figure 3(d) shows load distributions in a pile at various stages of construction, as well as those measured during the pile load test. The load test results were similar to those obtained from building loads but there was a notable difference near the pile toe. The building load, developing over several months, apparently caused higher end bearing force than that which had occurred during the short term pile load test.

Price & Wardle (1986) described a study carried out by BRE on the pile-raft foundation of an eleven storey building in Westminster, in order to determine the division of load between the raft and a bored pile. Load distribution along the pile length was not examined. Accurate bending moment at the pile top due to uplift of the raft (constructed in a 13.7 m deep excavation) was measured by means of sixteen sensing units at the same level. In most other cases, only two units were used at any level, and consequently any bending moments could not be properly measured.

2.2.3 Discussion

Most of the reported cases concern test piles. Bored cast-in-place piles and steel tube piles have been extensively studied. There is very little reported information on working driven concrete piles in buildings.

The most commonly used instruments have been strain gauges. A few studies have used photo-elastic glass (reviewed by Cooke, 1981) and tell-tale rods (Johannessen & Bjerrum, 1965; Rieke & Crowser, 1987). Two types of strain gauge have usually been used, namely electrical resistance (ER) and vibrating wire (VW) strain gauges. The operating principles of the two types are entirely different (see Hanna, 1973 and 1985). Cooke (1981) has mentioned some advantages of VW gauges, but stated that they are not obviously more reliable than ER gauges. He found in a BRE study, that a number of circuits of both types of gauge broke down after five years, but that some gauges of both types were still working. However, VW gauges have been used increasingly in recent studies (Leung & Radhakhrisnan, 1985; Price & Wardle, 1986; Sharma et al, 1986).

Many studies reported residual strains in piles (both compressive and tensile) after driving and after pile load testing (Keenan & Bozozuk, 1985; Ting & Toh, 1985; Albert et al, 1985). The significance of residual strains has been discussed by Rieke & Crowser (1987) and Poulos (1987). Poulos has also provided theoretical calculations which give residual tensile axial strains in driven piles under certain conditions. Apart from strains from axial forces, there could also be significant residual strains due to bending in driven piles, because the piles can never be driven perfectly straight and they may distort into helical curves with slight or sharp bends (Farid, 1981). However, most studies did not include a sufficient number of gauges (three or more in a section) for a proper determination of maximum strains due to bending. These residual strains may be 'locked in' for a long time, or may readjust themselves under changing load conditions (Cooke et al, 1979; Rieke & Crowser, 1987).

In Figure 2, the pile resistance during load test was mostly from skin friction, while the end bearing force was small. For shorter piles, the end bearing could be higher, and could provide greater resistance than the skin friction (Costa Nunes et al, 1985). In some cases, limit values of skin friction increased with time. The friction and axial force on a pile could be altered by disturbance due to the installation of adjacent piles (Cooke et al, 1979).

Positive friction is generally greater than negative friction in cohesionless soils, but they are approximately equal in medium to stiff clays (Broms, 1979; Mey et al, 1985). Broms also reported that small relative displacement in the order of a few millimetres can mobilize the maximum or limiting skin friction on a pile, while a large displacement, up to 20% of the pile diameter, is required to mobilize the maximum end bearing force.

2.3 Studies in Hong Kong

Lee (1979) discussed various methods used in Hong Kong to estimate negative skin friction, and presented a number of case studies from Hong Kong and elsewhere. Davies & Chan (1981) provided a general review of methods and techniques used in the design of piles in Hong Kong. They also summarised experience in Hong Kong of the use of piles in various situations.

Holt et al (1982) discussed tests on a 1.0 m diameter, 37 m long bored pile at a site near the Kowloon Bay Mass Transit Railway (MTR) station. The site has subsoil strata similar to those found at the site of the new Public Works Central Laboratory. The load test results gave positive frictional resistance averaged over the fill layer of about 30 kPa, while that for marine and alluvial deposits (not separated) was somewhat smaller. The value for weathered granite was more than 150 kPa.

Lee & Lumb (1982) carried out tests on 609 mm diameter, approximately 30 m long driven steel tube piles at a reclamation site in Tuen Mun. The development of negative skin friction was accelerated by construction of a 2 m high fill surcharge immediately after pile driving. The negative friction reached a maximum value after about six months, when the ground settlement was about 350 mm. The friction parameter β, see Appendix C.2, was estimated to be 0.61 for fill and 0.21 for marine clay, see also Figure 3(b). Comparison with another pile in the study, which was coated with bitumen, showed that the coating could reduce the negative friction force to only 14% of that for the uncoated pile.

The uncoated pile was subjected to load test after completion of the long term observation, and the results are shown in Figure 2(d). Most of the load was resisted by positive friction for the uncoated pile, while relatively low friction on the coated pile resulted in high end bearing force. Combining the test load with previously induced negative friction load, Lee & Lumb reported that the end bearing force on the normal pile was still higher than that on the coated pile by about 46%.

Evans (1987) and Evans et al (1987) discussed previous experience of using Daido piles, and compared the driving performance of the pile with those of three types of driven steel pile, through crushed rock fill reclamation. The conclusion from a number of cases was that the pile gives a satisfactory performance even under hard driving in cobbles or crushed rock fill. Its main attribute is the very high strength concrete used. The local manufacture of Daido piles began in July 1982, and they have been used increasingly in Hong Kong since that time. More than 7000 piles were driven in the one year period July 1983 to June 1984.

Franki Contractors Ltd. commissioned a number of field studies on the performance of Daido piles. Some tests which were carried out in the Kowloon Bay reclamation area are described below. A Fugro (HK) Ltd. report commissioned by Franki (ref. 83003, 1983) described dynamic pile testing on five 500 mm diameter Daido piles with 100 mm wall thickness. Dynamic skin friction and dynamic end resistance during driving were estimated to be 3500 kN and 2000 kN respectively at about 40 m depth. These were consistent with the values calculated from soil properties using the formulae for static loading. Reports by Test-consult CEBTP (FE) Ltd. commissioned by Franki (ref. R442-136/MSA/3 and /4, 1985) described tests on a pile of the same size. It had instruments at two levels only, attached on the surface at top and toe of the pile. Dynamic compressive stresses during driving were 45.5 and 9.9 MPa respectively. Test load was then applied to a maximum of 4600 kN and the compressive stresses at the same levels were 32 and 3 MPa respectively. They demonstrated that most of the load was resisted by positive skin friction.

The review has shown that there are relatively few reported cases of field studies on instrumented piles in Hong Kong. There are no reports of long term monitoring of driven concrete piles in buildings.

3. FIELDWORK

3.1 Site Description

The new Public Works Central Laboratory is located in the Kowloon Bay reclamation area, close to the Hong Kong International Airport and the Kwun Tong Typhoon Shelter, see location plan in Figure 4. Examination of aerial photographs revealed that reclamation work at this site was completed in 1967 (Lands Department Plate no. (11)-1967-5192). Therefore, the load from the fill on the subsoil strata has been maintained for about 20 years.

Four boreholes were drilled at this site by the Bachy Soletanche Group in 1983 as a part of the ground investigation for the building foundation design. The hole locations are given in Figure 4, the logs obtained are illustrated in Figure 5, and the soils are described in Figure 6. The site is underlain by fill, marine deposits, alluvium and weathered granite. Each of the first three layers is approximately 10 m thick. There are some variations of depths and thicknesses of the strata between the four holes. The logs indicate that the weathered granite rises to a higher level to the south. The SPT 'N' values are also shown in Figure 5. The presence of some sand in the marine clay may be indicative of disturbance and mixing with the fill during reclamation. In keeping with common practice, laboratory determinations and detailed descriptions of materials from the site were not made during the original ground investigation, and additional investigation was beyond the scope of this study.

In Figure 4, the locations of the seven instrumented piles are also shown. Three of them are situated in three separate pile groups (three piles in each group) and four of them are single piles. Two surface settlement points were established at the site to monitor long term settlement of the ground with respect to the pile tops and building.

3.2 Piles

The piles used for this building were manufactured by Daido Concrete (HK) Ltd. Instruments were installed in the piles during the casting process at the manufacturing plant in Tai Po.

The manufacturing processes are described as follows. The steel reinforcement is first placed in the lower half of a longitudinally split mould, and fresh concrete poured into the mould. After placing the upper part of the mould, the reinforcement is prestressed to give a prestress in the finished section of 5.25 MPa. The mould is then spun to create a centrifugal force of up to 35 g, forcing the concrete against the mould, and forming a central hollow. The pile is steam cured, removed from the mould and put into an autoclave at 194°C and 13 bar pressure. These operations are illustrated in Plates 2 to 5. The entire process takes less than one week. Pile sections are fabricated in lengths of 8 and 12 m. Steel end-plates permit on site welded connections between pile sections.

The characteristics of Daido piles were discussed by Evans (1987). The concrete was found to have ultimate strength of 78.5 MPa and allowable stress of 18.3 MPa, corresponding to allowable bearing capacity of 2700 kN and 2300 kN for piles with 125 mm thick walls and 100 mm thick walls (both 500 mm outside diameter) respectively. The allowable stress conforms to BS CP 2004 (BSI, 1972), now incorporated in BS8004 (BSI, 1986). The design load on each pile was based on this. The modulus of elasticity of the piles was determined to be 37.7 GPa.

Both 125 mm thick and 100 mm thick piles were used in this project. Two of the instrumented piles, nos 25A and 26A, were of the latter type while the other five were of the first type.

3.3 Strain Gauges

Two types of strain gauge, the ER type and VW type, were used in this study. The two types were used largely to provide an independent check, one against the other. The ER gauges were also a low cost supplement and back-up to the VW gauges. Operating principles were discussed by Hanna (1973 and 1985).

Two types of ER gauge, namely ER1 and ER2, were used. The ER1 gauges were OYO-ORH16B imported from Oyo Measurement Co Ltd., Japan through Daido Concrete Ltd. Each instrument consisted of one gauge (three-wire) mounted on a 25 mm diameter, 200 mm long steel bar with a threaded connection at each end to permit extension using two 17 mm diameter steel bars (see Figure 7). The larger steel bar was wrapped in heat-resistant plastic tape. The gauge was produced specifically for use in a high temperature autoclave. The three-wire technique was used to compensate for any changes in resistance in lead wires, see Kyowa (1985).

The ER2 gauges were constructed in-house as part of this study, using high temperature 'Kyowa' KFH-5-C1-11 foil gauges manufactured by Kyowa Electronic Instrument Co Ltd., Japan. Two gauges were attached at mid-length of a 12 mm diameter, 1.2 m long mild steel bar using Kyowa phenol based PC-6 gauge cement, and wrapped with PTFE tape before curing in an oven. The foil gauges were protected inside a concentric 19 mm diameter steel tube, held by two clamps, and the annular space was sealed with silicone-rubber (see Figure 7). The three-wire read out technique was used for both gauges, which shared two common wires.

The VW gauges used were TES/5.5, manufactured by Gage Technique Ltd., UK, and were obtained through Cedec Geotechnical Services (HK) Ltd. The vibrating wires used were especially treated by Gage Technique for this project to resist temperatures of up to 240°C.

The gauges were selected because of their ability to withstand the conditions during manufacture of the piles and pile driving, and their availability within the time schedule. ER1 gauges had been used in previous trials by Daido Concrete Ltd. in 1984. Pile no. 25A consisted of sections, containing ER1 gauges, which were cast at that time. The 'old' gauges embedded in these sections were tested before driving. ER2 and VW gauges were used for the first time in Daido piles in this study. Therefore, trial instrumentation and driving were carried out at an early stage to test the gauges, and pile no. 26A was used for this purpose. Piles nos 25A and 26A were the first two instrumented piles to be driven to test the whole process.

The measuring unit for all ER gauges was a portable Kyowa SDB-320, which was used in conjunction with a Kyowa SS-12R 12-channel switch-box. The unit used for the VW gauges was the portable Gage Technique GT1174. Both types were able to achieve theoretical accuracy of about one microstrain (i.e. changes in length of one part per million). The methods for calculation of strains from the readings are provided in Appendix C. In the field measurements, the resolutions achieved were estimated to be in the order of a few microstrains.

3.4 Installation of Gauges

Figure 7 shows an example of the pile instrumentation lay-out. The gauges were installed at five depths in each pile, at one depth each in three 8 m pile sections and at two depths in one 12 m section. At each depth, four gauges were distributed to three positions approximately equally spaced 120° apart. At depths other than the mid-depth, one ER2 gauge was set very close to the VW gauge for direct comparison of readings. At the mid-depth, this ER2 gauge was omitted. The three-position arrangement provided good estimates of bending strains. Since each ER2 contained two gauges, there were therefore six individual gauges at each depth except the mid-depth, where there were four.

The number of instrumented piles and the number of gauges in each pile were set higher than the minimum required to allow for possible losses of instruments in the short and long term. This also enabled better accuracy to be obtained in the calculation of stress and strain at each depth, and enabled comparison of results from similar piles.

The arrangements of gauges varied for individual piles. Those for piles nos 42, 63 and 118 were as illustrated in Figure 7. There were only four levels of instrumentation in pile no. 29, and the ER2 gauges near the VW gauges were replaced by trial four-gauge systems. Each of these formed a complete Wheatstone bridge, with a downhole amplifier to eliminate the masking effects of changes in resistance in the cables due to temperature changes. There were three gauges at each depth for pile no. 58. Piles nos 25A and 26A had gauges at only two positions, across the diameter at each level, instead of three. There were fewer VW and ER1 gauges in piles nos 58 and 26A, while pile no. 25A contained only ER1 gauges.

The dates of casting of the instrumented piles are given in Table 1. The strain gauges were attached to the reinforcement (Plate 1) and the heat resistant gauge cables ('Hiflon' FEP four-core cable) were laid along the reinforcement to the top of the pile section. After completion of the casting and curing processes, cables from gauges at each depth were joined to a 10-pair, 10 mm diameter telephone cable ('Hitachi', polyethylene, fully filled). There was, therefore, only one cable leading from each depth of instrumentation. At each depth all ER gauges shared two common wire pairs, while a separate circuit was provided for the VW gauge. The connection was protected with a 'Sigmaform' heat-shrink connector sealed with mastic.

The total number of gauges installed in this study was 115, consisting of 24 VW gauges, 44 ER1 gauges and 47 ER2 gauges.

3.5 Pile Driving

All piles were driven by Franki Contractors Ltd. They were driven section by section, each 8 m or 12 m long. The first section was equipped with a cone-shaped steel shoe. The next section was set upright and welded to the top of the previously driven section (Plate 9). The first two or three sections of all piles were driven using an RHI 45 (4.5 tonnes piston) diesel hammer. The remaining sections were driven to final depths by a heavier 'Delmag' D-62 (6.2 tonnes piston) diesel hammer. Driving dates of the instrumented piles are given in Table 1, together with their final depths.

A special dolly was used to let gauge cables pass through under the hammer. The cables from driven sections were threaded through the hollow of the section to be driven next, see Plate 8. The orientation of strain gauges in each pile section was recorded during driving. Driving was terminated when the rate of pile penetration satisfied the predetermined final set criterion. This was calculated using the Hiley formula (Bowles, 1982) and was dependent on pile length and temporary compression (eg. 28 mm per ten blows for a 44 m long, 125 mm thick pile, with 20 mm temporary compression allowed for the D-62 hammer without follower). Significant ground heave, in the order of 150 mm, was observed near each pile after driving. The hollow centres of all the instrumented piles were filled with concrete grout following driving to prevent ingress of water.

3.6 Discussion

There have been few previous attempts to install instruments in Daido piles (Section 2.3). Therefore, piles nos 25A and 26A were used specifically for initial testing purposes. During this stage a large proportion of the instruments were lost. The top instrumented pile sections of both piles had to be cut off because the final depths were about 8 m higher than expected, based on the depth determined from a probe pile. Other losses occurred during casting and driving, and as the result of flooding of the site during a rainstorm. Therefore, most of the gauges in pile no. 26A and about half of those in pile no. 25A were lost, i.e. gave either no reading or unstable (drifting) readings. It proved necessary to strengthen wire ties, improve joint water-proofing, raise the temperature rating of strain gauges and ensure careful pile handling on site.

As a result of these improvements, there were small losses for the remaining five piles. For all gauges in these piles, 6% were lost after casting and an additional 12% were damaged during pile driving. More than 80% were still functioning after pile installation. The losses were absorbed by the available redundancy. It is noted that the gauges were subjected to very harsh conditions during casting and driving. During these stages, the types of gauge in descending order of durability were VW, ER1 and ER2. It is expected that useful results will continue to be obtained from these gauges after two years, even if there are further losses of gauges in the long term.

3.7 Load Tests

Load tests on five piles, randomly selected, were carried out by Franki as a part of the piling contract. Three of the selected piles were instrumented piles, namely piles nos 118, 58 and 26A. The test on pile no. 58 was carried out from 25 to 28 May while those for piles nos 118 and 26A were conducted from 30 May to 2 June.

The tests were set up in the usual manner for the maintained load test. The top part of the pile was cut off below ground level and a small excavation formed around the pile to accommodate necessary equipment. The pile was jacked against a platform previously loaded with kentledge, using a hydraulic jack, see Plates 11 and 12. The applied load was read from a load gauge connected to the jack, and the settlement was measured from four dial gauges attached to a steel reference frame. The calculated settlement was the average of the four readings.

The load was applied in four cycles. The maximum load in each cycle was increased from half the design load to twice the design load. There was a brief pause at each load interval (half the design load), on both loading and unloading, to take settlement readings. The maximum test load was 5400 kN for piles nos 118 and 58 (125 mm wall thickness) and 4600 kN for pile no. 26A (100 mm wall thickness). The time taken for the four cycles was about two hours. The load was then maintained at the maximum value for three days before unloading to zero in four equal steps.

The strains in the instrumented piles were monitored throughout these load tests. Additional switch-boxes were constructed for this purpose to provide quick readings of a large number of gauges. Distribution of strains along the pile length allowed good estimation of the mobilized skin friction. The tests also provided data for a detailed assessment of strain gauge performance under field conditions. The results are discussed in detail below.

4. RESULTS AND ANALYSIS

4.1 Strain Gauge Responses

It is important to check that the strains obtained from strain gauge monitoring are consistent and reasonable (Broms, 1979 and Cooke, 1981). The best approach is to examine gauge response in working conditions under known loads.

The load tests provided the opportunity to examine the gauge response. A detailed assessment of the response from the different types of gauge during load testing is given in Appendix B. It was found that the VW and ER2 gauges gave identical readings, while the ER1 gauges consistently gave slightly higher readings. It was concluded that the ER1 gauge readings needed to be adjusted by a constant factor. The plot of strains obtained from the ER gauges against those obtained from the VW gauges is shown in Figure 8 (ER1 readings adjusted as above). The plot confirmed that the strains are consistent to within 5% in a range of up to 650 microstrains. The small deviations also showed that there was very little bending during the load test.

Changes in strain of about five microstrains or less can be readily detected in the load test.

An accurate value of modulus of elasticity of the pile is necessary for the conversion of the strains to stresses, and hence to axial forces. Bending tests on an instrumented pile section at the manufacturing plant confirmed the previously quoted value of 37.7 GPa. This test also demonstrated that the calculated strains and the measured strains were in good agreement. The modulus of elasticity of concrete grout in the pile hollow was determined by compression tests on cylindrical samples taken at the time of grouting. The value obtained was 11.5 GPa. Details of all the above tests are given in Appendix A.

Large temperature changes could affect strain gauge readings (Okabe, 1977; Lee & Lumb, 1982). Large changes occur near the ground surface, and diminish with increasing depth. In this study, the uppermost gauges were below 10 m depth to allow for cutting of the top pile section, and for the uncertainty of the final depth of the pile. Lee & Lumb reported that, at a site on the Tuen Mun reclamation, the temperature was fairly constant below 10 m depth, at about 24.3 $\pm$0.15°C. It was concluded, therefore, that there were negligible temperature effects on the gauges in this study.

4.2 Residual Strains

The strains were measured before and after driving of pile sections, and once every fortnight for two months after completion of driving. Typical results are illustrated in Figure 9. In each plot, the measured strains at the three gauge positions at a particular depth are shown. The strains were set to zero after casting of the piles. Hence, the strains reported in this section were additional to the strains induced by prestressing. It could be seen that large strains occurred after driving of each pile section, up to 1000 microstrains in the bottommost section. Some strains remained 'locked in' after completion of all driving. These residual strains were different at different gauge positions. The average of these strains at each depth was the axial strain, and the difference between each strain and the average was the bending strain. Relevant formulae are given in Appendix C.

Most of the pile sections had compressive residual axial strains, up to a value of about 200 microstrains. A few pile sections showed tensile residual axial strains (see Section 2.2.3) of less than 100 microstrains. The magnitudes of these strains varied in a random manner with depth, but the top pile sections generally had smaller residual strains. The maximum residual bending strains at these gauge positions were about 200 microstrains, corresponding to estimated locked-in moments greater than 100 kN-m. The random occurrence of axial and bending strains could be due to the driving process, in which the pile was not a single continuous member but consisted of about five sections driven at different times and in somewhat different positions relative to the driving machine.

Figure 9a shows the strain changes caused by test loading on pile no. 118. The strain changes were almost the same at the three gauge positions at each depth. The changes were smaller at greater depth. The load test results are discussed in the next section. The residual strains remained the same before and after test loading. Apparently, the strains at 19 m depth showed increasing compression with time. However, it was noted that the kentledge (almost 6000 kN) was left on the ground near this pile for several weeks before removal, and this may have caused the observed strains. No other piles showed similar strain changes. Therefore, it was concluded that no significant negative skin friction occurred at this site during the two month period.

4.3 Load Tests

The load test set-up is described in Section 3.7, and the results are presented in this section. The strains reported here were determined with reference to the initial zero strain condition at the time immediately before the test. Therefore, they were caused solely by the applied load during the test.

The measured pile strains during the load tests are shown in Figures 10 to 12 for piles nos 118, 58 and 26A respectively. The conventional load-settlement curves are given, together with the load-strain relationships at each gauge depth. The points on the loading paths are for the first-time loading, while those for reloading, having slightly larger settlements and strains, are omitted for clarity. All points on the unloading paths are included. Tables 2 and 3 show complete data for piles nos 118 and 58 respectively. The results from pile no. 26A will not be discussed further, due to the limited data obtained from this pile (Section 3.6). The strains presented here were the average of the strains from the gauges at each depth. A few obviously anomalous readings were excluded.

Using the moduli of elasticity for the pile and concrete grout (Appendix A) the strains were converted to axial forces in the piles, and are indicated on the scales on the right of Figures 10 and 11. At the maximum load, the axial forces at about 12 m and 40 m depth were about 4000 kN and 450 kN respectively, showing a large decrease in axial force with depth.

Figures 13 and 14 illustrate the decreasing strain and axial force with increasing depth. The four distributions were obtained at the maximum loads of the four loading cycles. The uppermost points were the applied loads, while all other points were derived from measured strains. The two sets of readings were correlated using the conversion discussed in Section 4.1 and Appendix A. The force distributions on the two piles were very similar, confirming the validity of the measurement for both piles. There were slight differences below 30 m depth, which could be due to the difference in level of the weathered granite surface at the two pile locations (Figures 13 and 14).

At the end of the pile load tests, after removal of load, locked-in strains remained in the piles, see Tables 2 and 3. It should be noted that the measured 'permanent settlements' of the pile tops were about 2 mm, about the same as the elastic shortening of the piles calculated from these locked-in strains. It is likely, therefore, that the permanent settlement usually obtained from a load test is not derived from pile tip penetration into the ground, but simply from locked-in elastic shortening of the pile.

The force distributions obtained here were typical of cases in which positive friction is mobilized to resist most of the applied load, see Section 2.1, Figures 1 and 2. Measurements at the greatest gauge depths, 4 m above the pile tip, showed that the end bearing force was less than 450 kN, or less than 10% of the applied load. Therefore, more than 90% of the load was taken up by skin friction during the pile load tests.

4.4 Skin Friction

The unit frictional resistance was calculated from the difference in axial forces at two gauge levels divided by the appropriate pile surface area (Section 2.1). The estimated unit friction mobilized over different depth ranges was plotted against relative displacements between the pile and the surrounding soil in Figures 15 and 16.

The displacements were estimated from the cumulative elastic shortening of the piles, which was calculated from the measured strains in Tables 2 and 3. The calculated shortening at the pile tops, under maximum test load, was about 2 mm (10%) less than the settlements measured from the dial gauges. Within the accuracy of this type of comparison, it cannot be ascertained whether all of the excess 2 mm was actually due to pile tip penetration. It was assumed, therefore, that the pile tip penetration was small, and that the relative displacement was due to elastic shortening only.

The instrument levels were sufficiently close to the interfaces between soil strata to allow estimation of the skin friction in each of the strata. At approximately the same relative displacement, the unit friction was high for weathered granite, low for marine clay, and intermediate between the two for other soils, see Figures 15 and 16. The flattening of unit friction-displacement curves after an initial steep rise indicates that the friction was approaching full mobilization at displacement greater than 5 mm. At this displacement the average unit friction was about 80 kPa for fill, 65 to 95 kPa for alluvium and 45 kPa for marine clay. The high friction in the marine clay in pile no. 58, 80 kPa, could have been due to mixing with the fill layer, and therefore it is not included in the estimate. For weathered granite, the bottommost layer, the displacement was small and the skin friction curve did not show any flattening. Therefore, the friction was considered far from fully mobilized, even though it was calculated to have reached more than 100 kPa.

At the maximum test load, the average frictional resistance over the full length of the pile was about 75 kPa. Initial estimates for positive friction parameter β (Appendix C) were 1.0 for fill, 0.25 for marine clay and 0.35 for alluvium.

4.5 Pile Resistance and Load

Load-settlement relationships obtained from the load tests appeared to show satisfactory performance of piles under twice the design load. However, the strain measurements indicated that most of the pile resistance was due to positive friction. It is anticipated that in the long term there may be settlements in the marine clay due to possible changes in water table, dissipation of pore pressure built up during pile driving, and secondary compression. Therefore, the positive friction in the fill and marine clay layers cannot be relied upon in estimating pile resistance and, in fact, negative friction may occur, resulting in additional load on the piles. This may induce higher end bearing forces and larger pile settlements than those which occurred during the load tests. Consequently, the load-settlement curves obtained from the load tests may be quite different from the long term pile performance as required in the design.

A more representative assessment is made below on the basis of the skin frictions and end forces obtained from the initial stage of this study, supplemented by those taken from other similar field studies on piles in Hong Kong (Section 2.3). It is important to reassess the performance independently from the initial design and final set criteria, which were based on calculations using conventional formulae. This assessment will be verified by continued monitoring of the piles under this project.

4.5.1 Pile Resistance

Pile resistance consists of end bearing force and positive skin friction (Section 2 and Figures 1 and 3). It is expected that positive skin friction will be developed in alluvium and weathered granite, and that the neutral point will be near the interface between marine clay and alluvium.

This study estimated the positive friction in weathered granite, not yet fully mobilized, to be more than 100 kPa. The value reported by Holt et al (1982) was more than 150 kPa. The latter value was used in the following calculation. No previous estimates were found for alluvium. This study gave a range of 65 to 95 kPa. The lower value was used. The thicknesses of the two soil layers were taken to be 8 m and 11 m respectively, and the combined positive friction for the two layers was calculated to be 3000 kN. During the load tests the positive friction in these layers, not yet fully mobilized, was about 2500 kN.

The end bearing layer is weathered granite. This may be assumed to be a cohesionless soil in which end resistance pressure can be found from p'Nq, where p' is the effective overburden pressure and Nq is the bearing capacity factor (Tomlinson, 1977). At the depth of the pile tip, SPT 'N' values were greater than 30, corresponding to a friction angle of about 35° (Peck, Hanson & Thornburn, 1974), and Nq values variously quoted to be from 45 to 250 (Tomlinson, 1977; Bowles, 1982; Fleming et al, 1985). Using the low value, the bearing pressure was calculated to be about 17 MPa at 43 m depth. However, this pressure exceeded the limit of 10.7 MPa specified by Tomlinson and by Fleming et al, who stated that higher pressure may induce excessive settlement. Using the limit pressure, end resistance was estimated to be 2100 kN. This value was similar to the dynamic end resistance of about 2000 kN found in the Fugro study reviewed in Section 2.3. In comparison, the mobilized end resistance at maximum test load in this study was less than 450 kN.

The total available pile resistance combining positive friction and end bearing is therefore 5100 kN. This is considered the minimum available pile resistance.

4.5.2 Pile Load

The assumed pile load consists of working load and negative friction load. The working load, including building load (dead load and live load) was taken to be not more than 1700 kN per pile in the design for this building.

Negative skin friction could occur in the marine deposits and fill layer. At this stage only positive friction has been determined in this study. The values determined for positive friction may be taken as an upper bound, since negative friction is normally less than positive friction (Broms, 1979). From the Lee & Lumb (1982) study on a steel pile (Section 2.3), the average fully mobilized negative friction was about 50 kPa for fill and 40 kPa for marine clay, corresponding to β values of 0.61 and 0.21 respectively. The thicknesses of the two layers at the Kowloon Bay site were about 11 m each, the top 2 m cut-off being deducted from the fill thickness. Using the negative friction values of Lee & Lumb as a maximum limit for the case of very large settlement, the total negative friction for the two layers was estimated to be 1550 kN.

Therefore, the total pile load including working load and negative friction load is not more than 3250 kN.

4.5.3 Discussion

The comparison of possible maximum load to minimum available pile resistance demonstrates the adequacy of the piles in the worst case. In fact, the piles may retain a large reserve load capacity if only small negative skin friction is developed in the future. Long term monitoring of the instrumented piles under this project should resolve this question. Comparative data from a new project at To Kwa Wan (Williams, 1987) will also assist in the future determination of skin friction development.

The working load given in Section 4.5.2 was for a 125 mm thick pile. The load for a 100 mm thick pile was lower, i.e. about 1300 kN. Since outside diameters of both types of pile are the same, other forces are also applicable to the thin pile. Therefore, the above conclusions are also valid for this type of pile, and the stresses should be comparable to those in the 125 mm thick piles.

It is emphasized here that the negative friction values used are for a fully mobilized state,, when large settlement has occurred (more than 350 mm, induced by a new fill surcharge 2 m high, see Lee & Lumb, 1982). The Kowloon Bay reclamation is 20 years old, and the settlement is expected to be less than this. Therefore, the actual negative skin friction is anticipated to be less than the fully mobilized value, although at this stage it is not possible to assign a value. However, it is also noted that negative friction on the smoother surface of the steel pile studied by Lee & Lumb may be less than that on the concrete piles which are the subject of this study (Tomlinson, 1977).

The weathered granite can be expected to provide higher resistance than purely cohesionless soils such as sand and gravel. In a weathered granite profile, strength will normally increase gradually with increasing depth. It could be expected, therefore, that the actual end resistance is higher than the estimate, and that the limit bearing pressure of 10.7 MPa for cohesionless soil (Tomlinson, 1977) is unduly conservative for weathered granite. A load test using constant rate of penetration to a very high load, with instruments for measuring the end resistance, should be able to provide a more realistic estimate of end bearing capacity than the maintained load test, at twice the design load, used in this case. Good estimation of the end bearing capacity is important in the design of piles which will be subjected to negative skin friction.

5. CONCLUSIONS

(a) Instrumentation has been installed on seven working piles of the new Public Works Central Laboratory, and initial results reported. Load tests on the instrumented piles verified satisfactory performance of the gauges used, and demonstrated the adequacy of the instrumentation techniques.

(b) There were significant residual strains in the piles after completion of pile driving. These included both axial and bending strains.

(c) The load tests provided good estimates of mobilized positive skin friction for the soil strata encountered. The average friction over the full pile length was about 75 kPa at maximum load. During load testing, the skin friction constituted most of the pile resistance, while the end bearing force was less than 10% of the total applied load.

(d) The initial assessment indicates that the piles will give satisfactory functional performance, even in the event of full mobilization of negative skin friction. Long term observation of the piles will determine the actual magnitude of negative skin friction developed. This data, together with data to be obtained from a new project at To Kwa Wan, should greatly assist in the future prediction of skin friction development on piles.

6. REFERENCES

Albert, L.F., Rocchi, G.F., Varisco, D. & Veronelli, P. (1985). Remarks on instrumented driving for offshore platform piles. Proceedings of the Eleventh International Conference on Soil Mechanics and Foundation Engineering, San Francisco, vol. 3, pp 11-16.

Bowles, J.E. (1982). Foundation Analysis and Design. (Third Edition). McGraw-Hill Inc., Singapore, 816 p.

BSI (1972). Code of Practice for Foundations. (CP 2004:1972). British Standards Institution, London, 158 p.

BSI (1986). Foundations. (BS 8004:1986). British Standards Institution, London, 160 p.

Broms, B. (1979). Negative skin friction. Proceedings of the Sixth Asian Regional Conference on Soil Mechanics and Foundation Engineering, Singapore, vol. 2, pp 41-76.

Buttling, S. (1976). Estimates of shaft and end loads in piles in chalk using strain gauge instrumentation. Geotechnique, vol. 26, pp 133-147.

Cooke, R.W. (1981). Instrumented piles and pile groups. Piles and Foundations, edited by F.E. Young, pp 166-172, Thomas Telford Ltd., London.

Cooke, R.W., Price, G. & Tarr, K. (1979). Jacked piles in London Clay : a study of load transfer and settlement under working conditions. Geotechnique, vol. 29, pp 113-147.

Costa Nunes, A.J., Golombek, S., Okay, M., Tavora Pinho, J.C. & Bichara, M. (1985). Load tests and load transfer on short bored piles. Proceedings of the Eleventh International Conference on Soil Mechanics and Foundation Engineering, San Francisco, vol. 3, pp 1369-1372.

Davies, R.V. & Chan A.K.C. (1981). Pile design in Hong Kong. Hong Kong Engineer, vol. 9, no. 3, pp 21-28.

Evans, G.L. (1987). The performance of driven prestressed concrete piles. Hong Kong Engineer, vol. 15, no. 3, pp 9-16.

Evans, G.L., Wong, P.P. & Sanders, H. (1987). The performance of driven piles in a crushed-rock-filled reclamation. Hong Kong Engineer, vol. 15, no. 4, pp 29-42.

Farid, M.U. (1981). Dynamic and static stresses in steel H piles. Piles and Foundations, edited by F.E. Young, pp 46-58, Thomas Telford Ltd., London.

Fleming, W.G.K., Weltman, A.J., Randolph, M.F. & Elson, W.K. (1985). Piling Engineering. Surrey University Press, London, 380 p.

Fukuya, T., Todoroki, T. & Kasuga, M. (1982). Reduction of negative skin friction with steel tube NF pile. Proceedings of the Seventh Southeast Asian Geotechnical Conference, Hong Kong, pp 333-347.

Granet, I. (1980). Strength of Materials for Engineering Technology. (Second edition). Prentice-Hall Co., Virginia, 483 p.

Hanna, T.H. (1973). Foundation Instrumentation. Trans Tech Publications, Clausthal, 372 p.

Hanna, T.H. (1985). Field Instrumentation in Geotechnical Engineering. Trans Tech Publications, Clausthal-Zellerfeld, 843 p.

Holt, D.N., Lumb, P. & Wong, P.K.K. (1982). Site control and testing of bored piles at Telford Gardens an elevated township at Kowloon Bay, Hong Kong. Proceedings of the Seventh Southeast Asian Geotechnical Conference, Hong Kong, pp 349-361.

Johannessen, I.J. & Bjerrum, L. (1965). Measurement of the compression of a steel pile to rock due to settlement of the surrounding clay. Proceedings of the Sixth International Conference on Soil Mechanics and Foundation Engineering, Montreal, vol. 2, pp 261-264.

Karlsrud, K. & Haugen, T. (1985). Axial static capacity of steel model piles in over-consolidated clay. Proceedings of the Eleventh International Conference on Soil Mechanics and Foundation Engineering, San Francisco, vol. 3, pp 1401-1406.

Keenan, G.H. & Bozozuk, M. (1985). Down drag on a three-pile group of pipe piles. Proceedings of the Eleventh International Conference on Soil Mechanics and Foundation Engineering, San Francisco, vol. 3, pp 1407-1412.

Kyowa (1985). Strain Gauge Instruction Manual. Kyowa Electronic Instrument Co. Ltd., Tokyo, 42p.

Konrad, J.M. & Roy, M. (1987). Bearing capacity of friction piles in marine clay. Geotechnique, vol. 37, pp 163-175.

Lee, P.K.K. (1979). Negative skin friction on piles. Asian Architect and Builder, vol. 8, no. 1, pp 31-35.

Lee, P.K.K. & Lumb, P. (1982). Field measurements of negative skin friction on steel tube piles in Hong Kong. Proceedings of the Seventh Southeast Asian Geotechnical Conference, Hong Kong, pp 363-374.

Leung, C.F. & Radhakrishnan, R. (1985). The behaviour of a pile-raft foundation in weak rock. Proceedings of the Eleventh International Conference on Soil Mechanics and Foundation Engineering, San Francisco, vol. 3, pp 1429-1432.

Mallard, D.J. & Ballantyne, J.L. (1976). The behaviour of piles in Upper Chalk at Littlebrook D Power Station. Geotechnique, vol. 26, pp 115-132.

Mey, R., Oteo, C.S., Sanchez del Rio, J. & Soriano, A. (1985). Field testing on large driven piles. Proceedings of the Eleventh International Conference on Soil Mechanics and Foundation Engineering, San Francisco, vol. 3, pp 1559-1564.

Okabe, T. (1977). Large negative friction and friction-free pile methods. Proceedings of 0the Ninth International Conference on Soil Mechanics and Foundation Engineering, Tokyo, vol. 2, pp 679-682.

Peck, R.B., Hanson, W.E. & Thornburn, T.H. (1974). Foundation Engineering. (Second edition). John Wiley, New York, 310 p.

Poulos, H.G. (1987). Analysis of residual stress effects in piles. Journal of Geotechnical Engineering, American Society of Civil Engineers, vol. 113, no. 3, pp 216-229.

Price, G. & Wardle, I.F. (1986). Queen Elizabeth II Conference Centre : monitoring of load sharing between piles and raft. Proceedings of the Institution of Civil Engineers, Part I, vol. 80, pp 1505-1518.

Rieke, R.D. & Crowser, J.C. (1987). Interpretation of pile load test considering residual stresses. Journal of Geotechnical Engineering, American Society of Civil Engineers, vol. 113, no. 4, pp 320-349.

Sharma, H.D., Harris, M.C., Scott, J.D. & Mcallister, K.W. (1986). Bearing capacity of bored cast-in-place concrete piles on oil sand. Journal of Geotechnical Engineering, American Society of Civil Engineers, vol. 112, no. 12, pp 1101-1116.

Shibata, T., Sekiguchi, H. & Yukimoto, H. (1982). Model test and analysis of negative friction acting on piles. Soils and Foundations, vol. 22, no. 2, pp 29-39.

Ting, W.H. & Toh, C.T. (1985). An instrumented bored pile with soil improvement for increased shaft resistance. Proceedings of the Eleventh International Conference on Soil Mechanics and Foundation Engineering, San Francisco, vol. 3, pp 1483-1488.

Tomlinson, M.J. (1977). Pile Design and Construction Practice. Cement and Concrete Association, London, 413 p.

Williams, J.A. (1987). GCO Internal Report - Proposed AOM HQ/Kowloon Depot, To Kwa Wan Reclamation. Preliminary Geotechnical Assessment Report PGA 6/87, Geotechnical Unit, Architectural Services Department, Hong Kong, 63 p.

Yong, K.Y., Cheah, W.B. & Yap, N.C. (1982). Ultimate load test of an instrumented cast-in-situ bored pile installed in stiff silty clay. Proceedings of the Seventh Southeast Asian Geotechnical Conference, Hong Kong, pp 453-463.

LIST OF TABLES

Table 1 - Dates of Casting and Driving, and Final Depths of Instrumented Piles

Pile No.	Dates of Casting	Dates of Driving		Final Depth below Ground (metres)
		Start	Finish	
25A	*	30 Mar	15 Apr	36.3
26A	13 Mar	2 Apr	16 Apr	35.9
29	23 Apr	4 May	7 May	42.9
42	13 Apr	4 May	13 May	43.4
58	8 Apr	4 May	9 May	43.8
63	16 Apr	4 May	13 May	43.5
118	22 Apr	4 May	8 May	42.6

Legend :

* Pile instrumented and cast in 1984 by Daido Concrete (HK) Ltd.. All others instrumented and cast in 1987.

A Indicates 100mm wall thickness. All others have 125mm wall thickness.

Table 2 - Load, Settlement and Compressive Strains in Pile from Load Test on Pile No. 118

Date	Time Hr:Min	Load (kN)	Settlement (mm)	Compressive Strain in Pile (microstrain) at Depth below Ground				
				11 m	19 m	23 m	31 m	39 m
30.05.87	09:12	0	0	0	0	0	0	0
	09:16	1350	3.08	91	41	29	14	3
	09:20	0	-0.04	-5	-2	-2	0	0
	09:26	1350	3.05	105	60	36	17	6
	09:33	2700	7.81	273	192	124	22	15
	09:37	1350	4.77	169	119	80	47	10
	09:41	0	0.11	-2	2	4	4	-1
	09:45	1350	3.32	116	69	43	17	6
	09:49	2700	7.91	276	191	126	65	15
	09:55	4050	14.13	458	364	275	176	41
	09:58	2700	11.43	366	301	236	157	36
	10:01	1350	6.76	201	178	147	107	24
	10:05	0	0.36	0	10	10	20	4
	10:12	1350	3.58	112	73	50	37	8
	10:17	2700	8.36	279	200	138	83	19
	10:22	4050	14.23	460	366	277	176	41
	10:29	5400	20.75	636	532	432	307	77
	10:33	4050	15.37	554	478	397	278	72
	10:37	2700	14.23	408	365	318	193	61
	10:40	1350	8.49	225	207	193	170	41
	10:45	0	0.78	1	14	21	28	8
	11:01	5400	21.35	647	545	448	322	81
02.06.87	13:41	5400	21.91	664	590	467	341	78
	13:43	4050	19.88	596	548	444	331	75
	13:47	2700	16.02	455	448	372	296	65
	13:51	1350	10.52	268	294	276	234	49
	13:57	0	2.67	-	94	82	72	17
	14:42	0	-	30	81	74	85	15

Table 3 - Load, Settlement and Compressive Strains in Pile from Load Test on Pile No. 58

Date	Time Hr:Min	Load (kN)	Settlement (mm)	Compressive Strain in Pile (microstrain) at Depth below Ground				
				12 m	20 m	24 m	32 m	40 m
25.05.87	09:25	0	0	0	0	0	0	0
	09:58	1350	2.65	–	38	24	8	2
	10:01	0	0.01	–	4	1	1	-1
	10:06	1350	2.65	–	35	25	7	2
	10:10	2700	6.87	245	131	88	27	10
	10:13	1350	4.65	167	94	65	19	7
	10:18	0	0.16	6	3	5	3	1
	10:22	1350	2.78	90	40	28	9	3
	10:26	2700	6.91	245	131	89	27	10
	10:33	4050	11.89	424	267	193	65	26
	10:36	2700	10.29	366	240	176	60	25
	10:39	1350	6.34	225	156	118	42	17
	10:41	0	0.33	9	5	10	7	3
	10:44	1350	3.23	100	47	36	15	6
	10:50	2700	7.24	255	140	101	33	13
	10:55	4050	11.98	425	270	196	66	27
	11:01	5400	18.15	619	430	337	137	60
	11:03	4050	16.67	566	406	322	133	58
	11:06	2700	13.12	440	330	269	116	52
	11:08	1350	7.5	256	205	174	81	36
	11:11	0	0.42	13	9	19	17	8
	11:27	5400	18.49	626	440	347	140	61
28.05.87	13:06	5400	18.99	645	474	403	179	64
	13:40	4050	18.13	620	445	374	149	46
	13:42	2700	14.85	504	378	332	137	42
	13:45	1350	9.91	333	250	241	109	32
	13:50	0	2.04	78	43	78	45	6
	14:00	0	1.85	–	–	–	–	–

LIST OF FIGURES

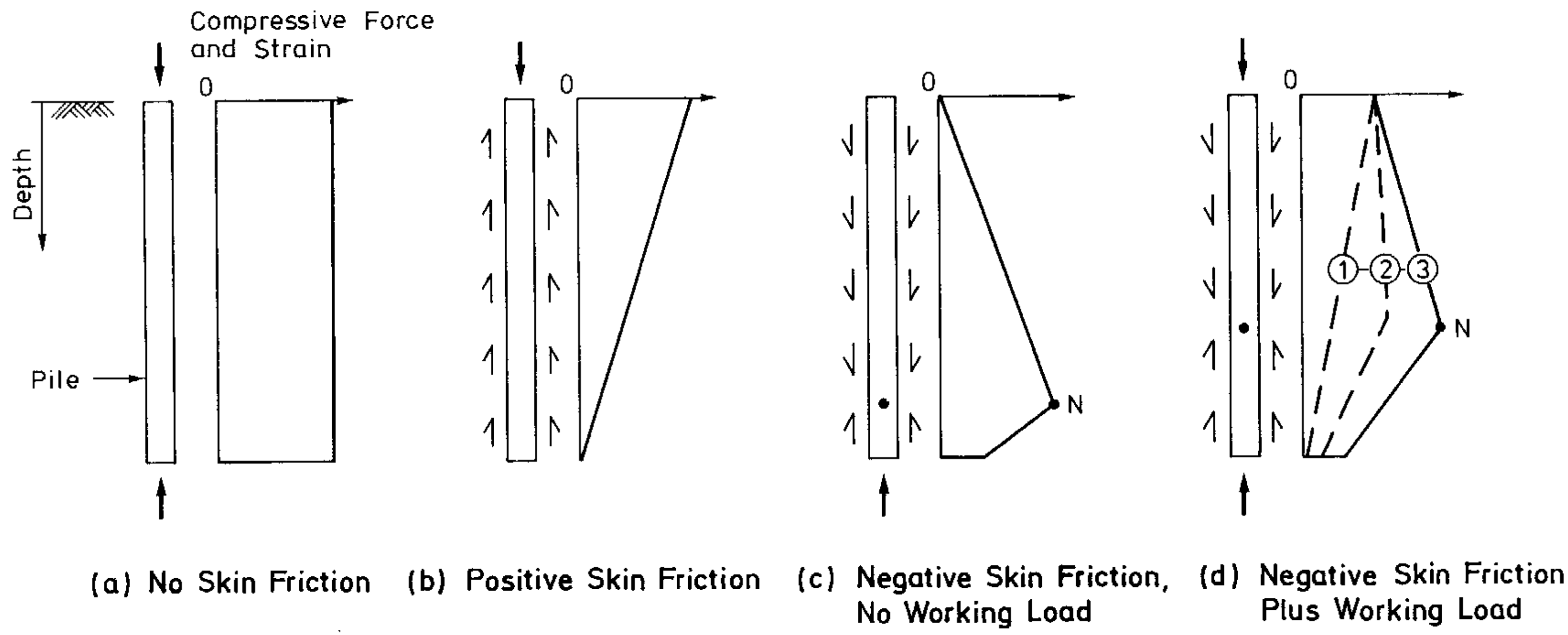

Notes : (1) N is neutral point separating zone of negative friction from zone of positive friction.
(2) ① ② ③ indicates expected development of negative friction with time.

Figure 1 - Hypothetical Distributions of Compressive Force and Strain in a Pile under Different Loading Conditions

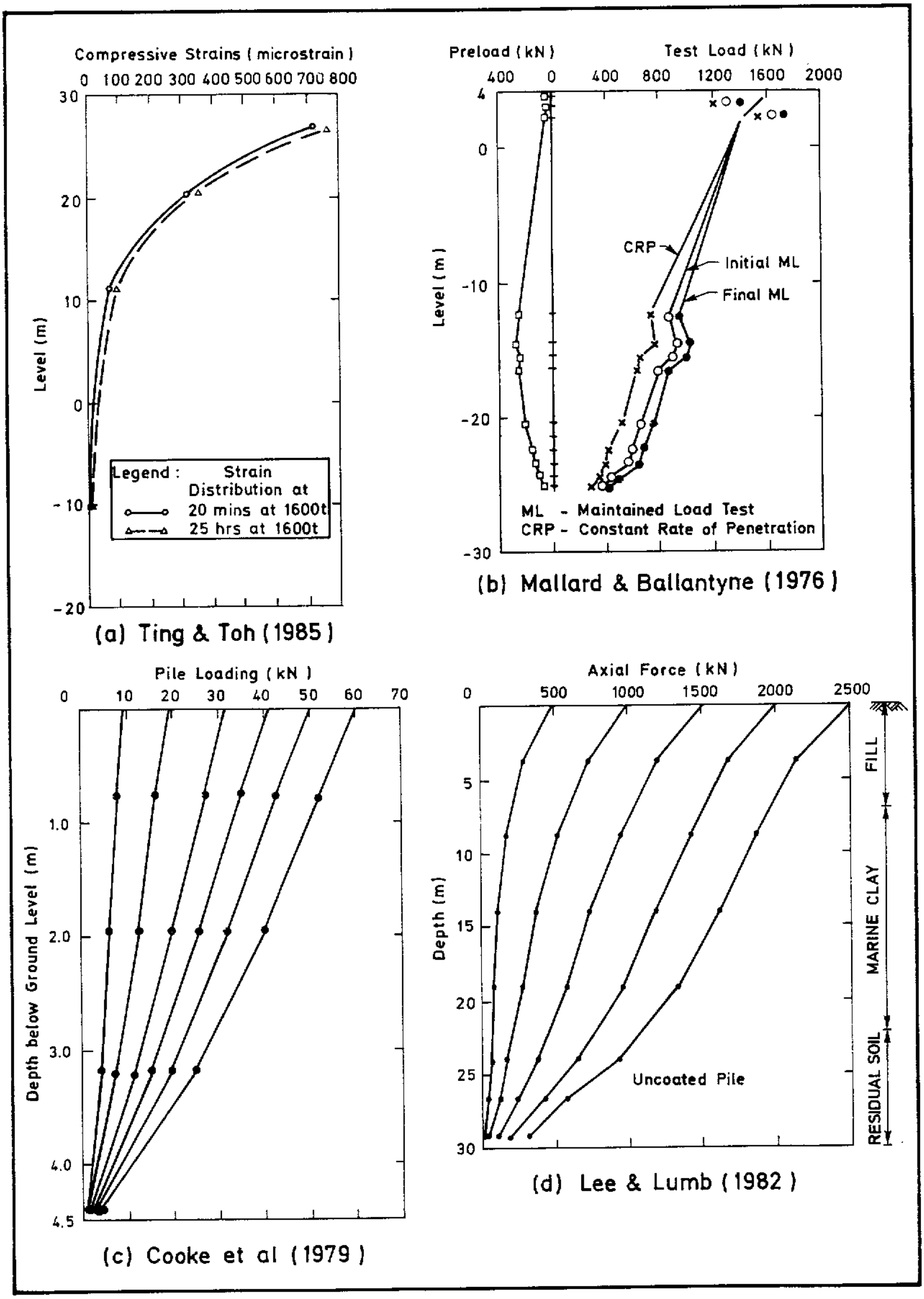

Figure 2 - Previous Studies on Strain/Force Distribution during Load Tests on Instrumented Piles

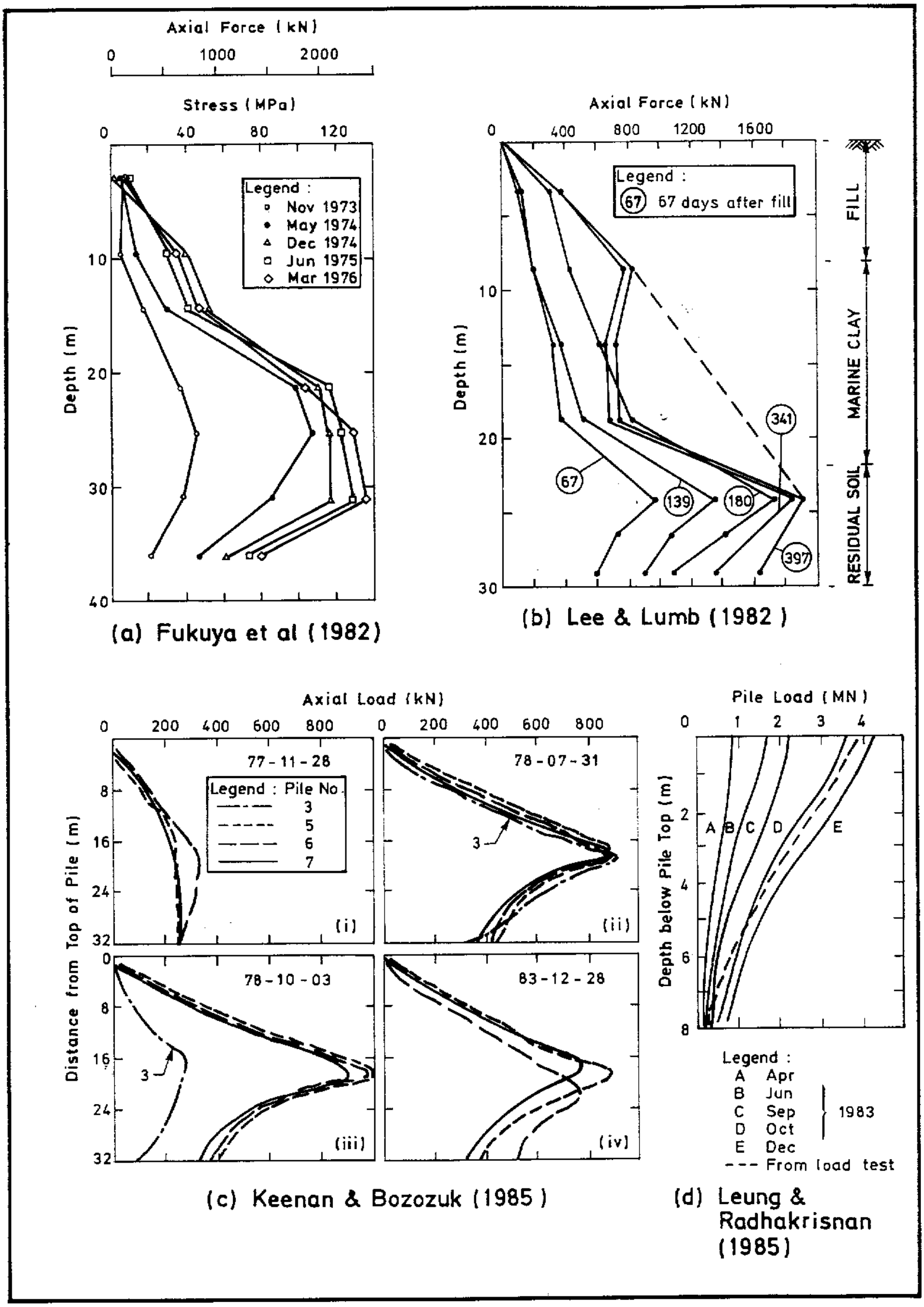

Figure 3 - Previous Studies on Long Term Changes in Strain/Force Distribution in Piles: (a) to (c) Negative Skin Friction, (d) Construction Loads

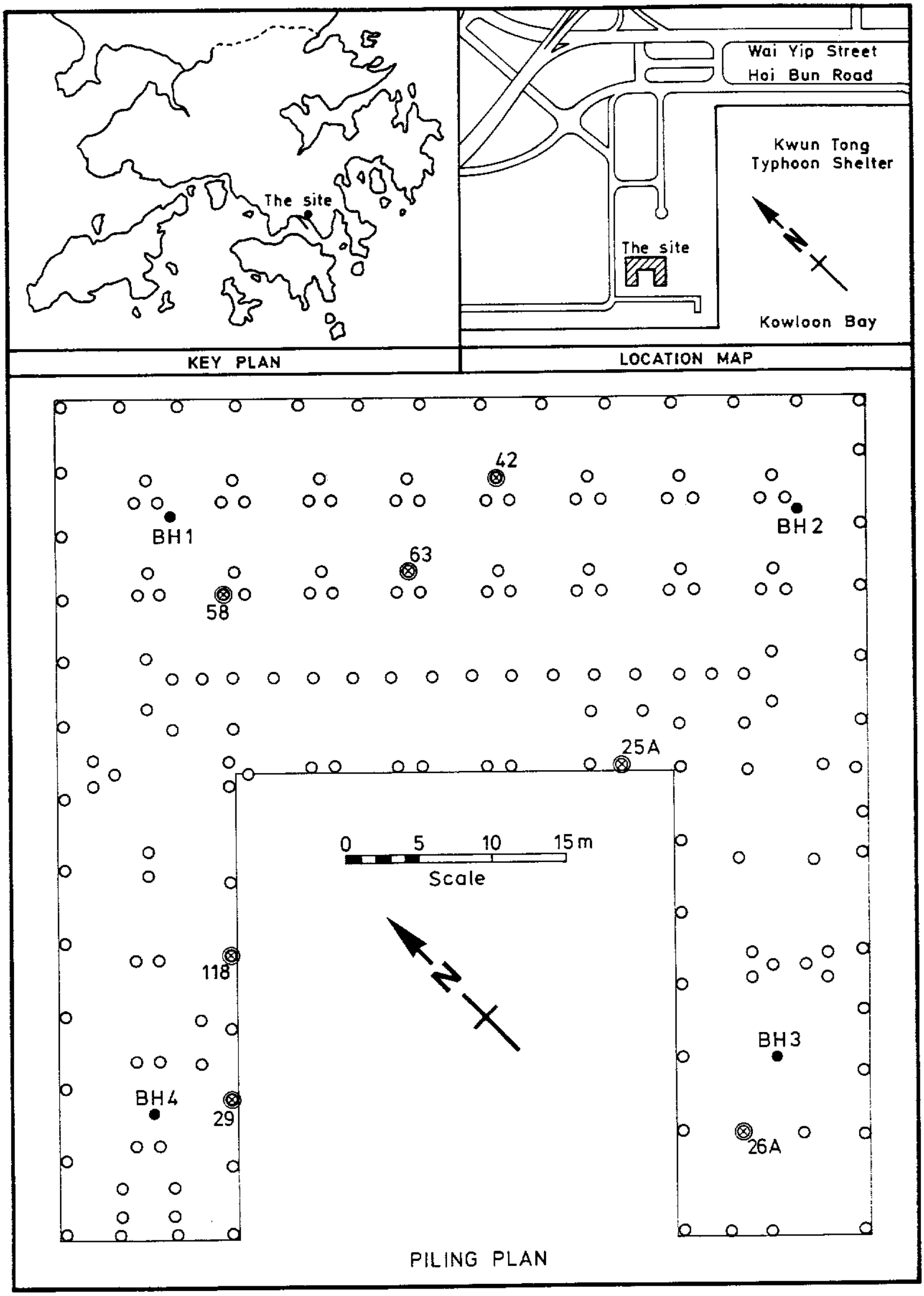

Figure 4 - Piling Plan of the New Public Works Central Laboratory Showing Locations of Instrumented Piles and Boreholes

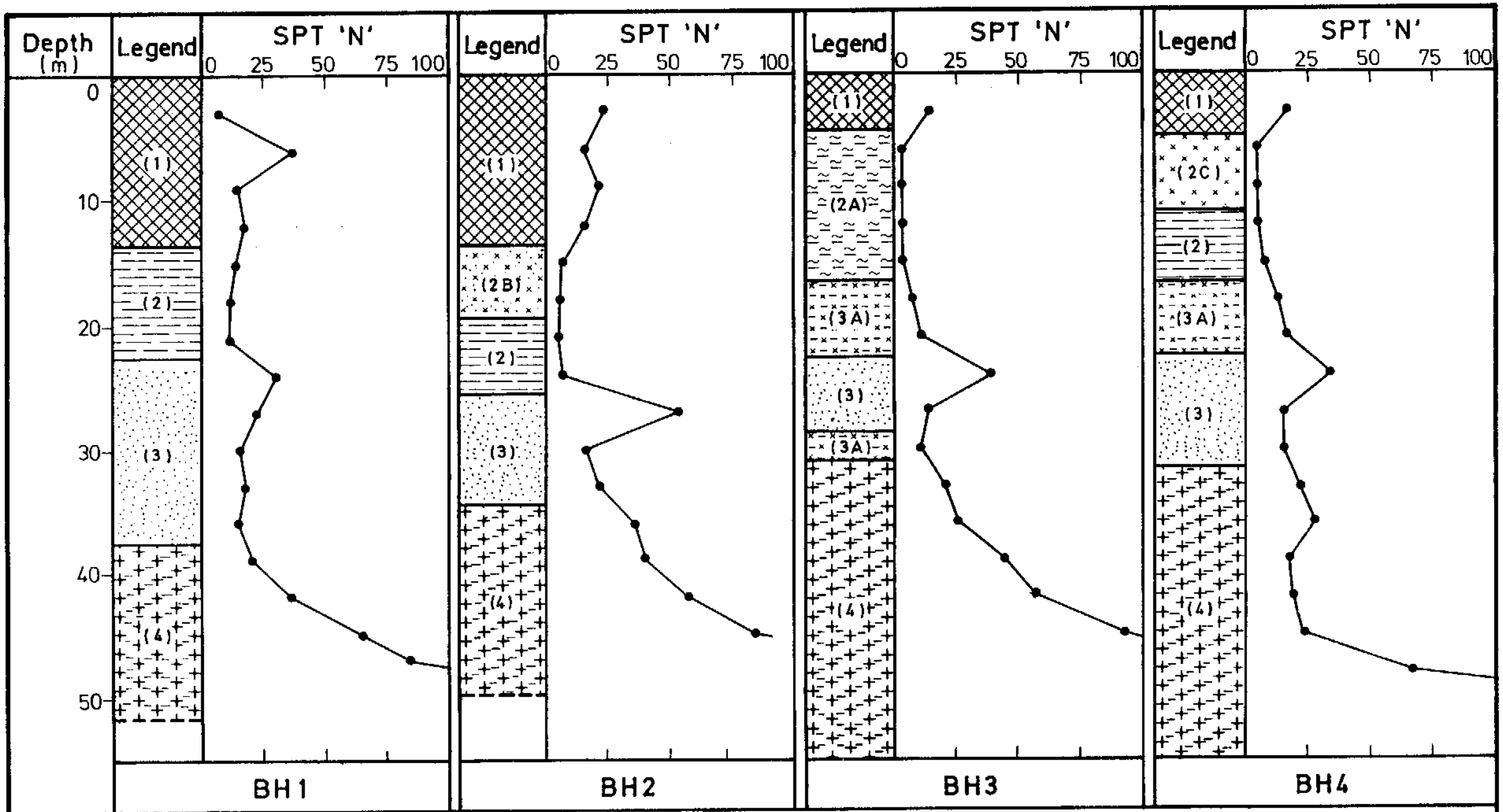

Notes : (a) Ground investigation was carried out by Bachy Soletanche.
(b) See soil legend in Figure 6.
(c) See location of bore holes in Figure 4.
(d) SPT 'N' is no. of blows per 300mm penetration.

Figure 5 - Borehole Logs and SPT Values at the Site, after Record by Bachy Soletanche Group, 1983

Legend	Description	
	(1) Medium dense, fine to coarse SAND with gravel and cobbles	(FILL)
	(2) Firm to stiff, silty CLAY with traces of sand and shell fragments	(MARINE DEPOSITS)
	(2A) Soft, silty CLAY with traces of sand and shell fragments	
	(2B) Fine to medium, silty, clayey SAND with fine gravel and traces of shell fragments	
	(2C) Firm, fine, sandy, clayey SILT	
	(3) Medium dense, fine to coarse SAND with fine gravel	(ALLUVIUM)
	(3A) Firm to stiff, silty CLAY with traces of sand and fine gravel	
	(4) Medium dense to dense, medium to coarse, clayey, silty SAND	(WEATHERED GRANITE)

Figure 6 - Description of Soil Strata at the Site, after Record by Bachy Soletanche Group, 1983

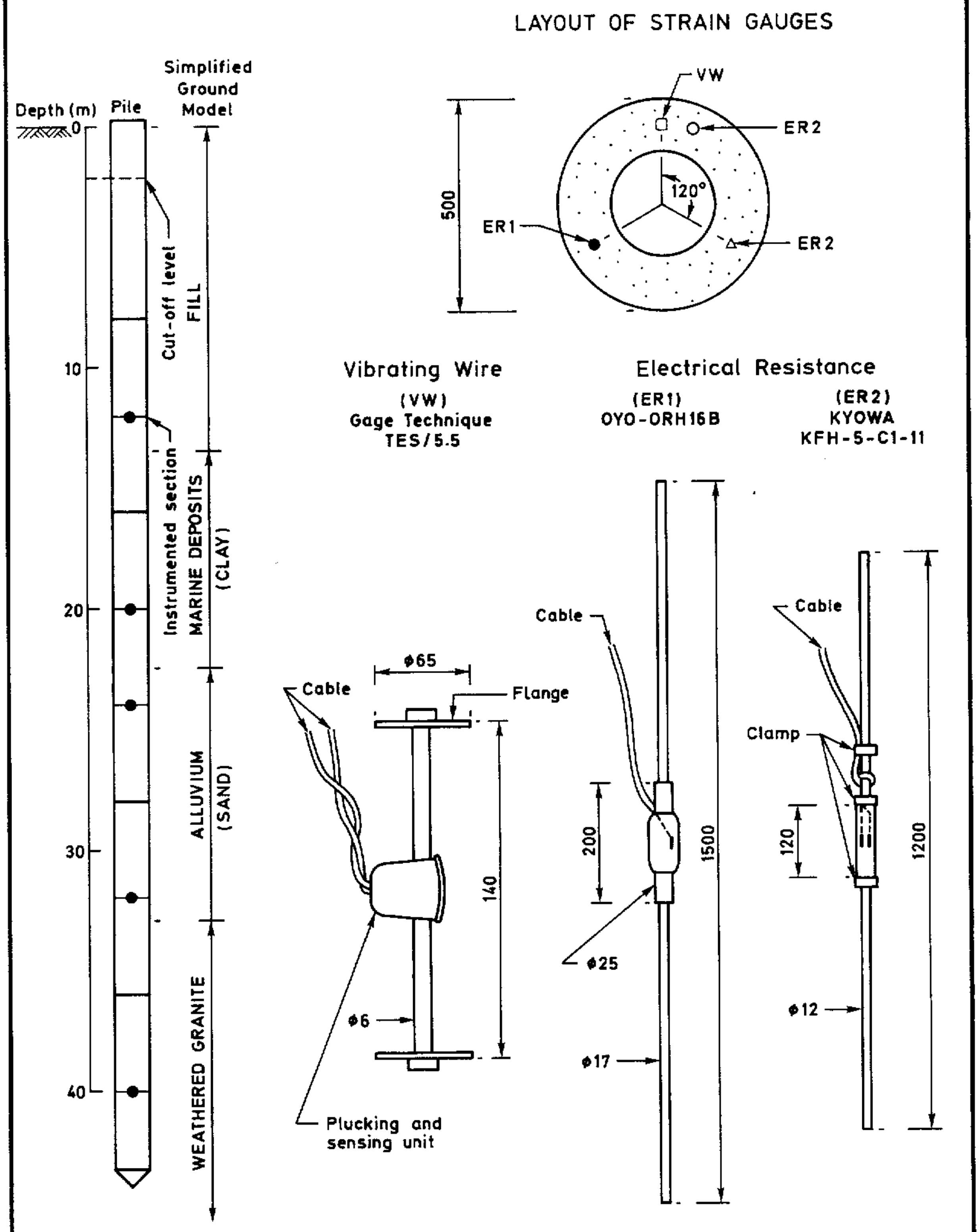

Notes : (1) All dimensions are in millimetres except depth below ground.
(2) Arrangements for individual piles vary from this example.
(3) See description of strain gauges in Section 3.3.

Figure 7 - Details of Pile Instrumentation

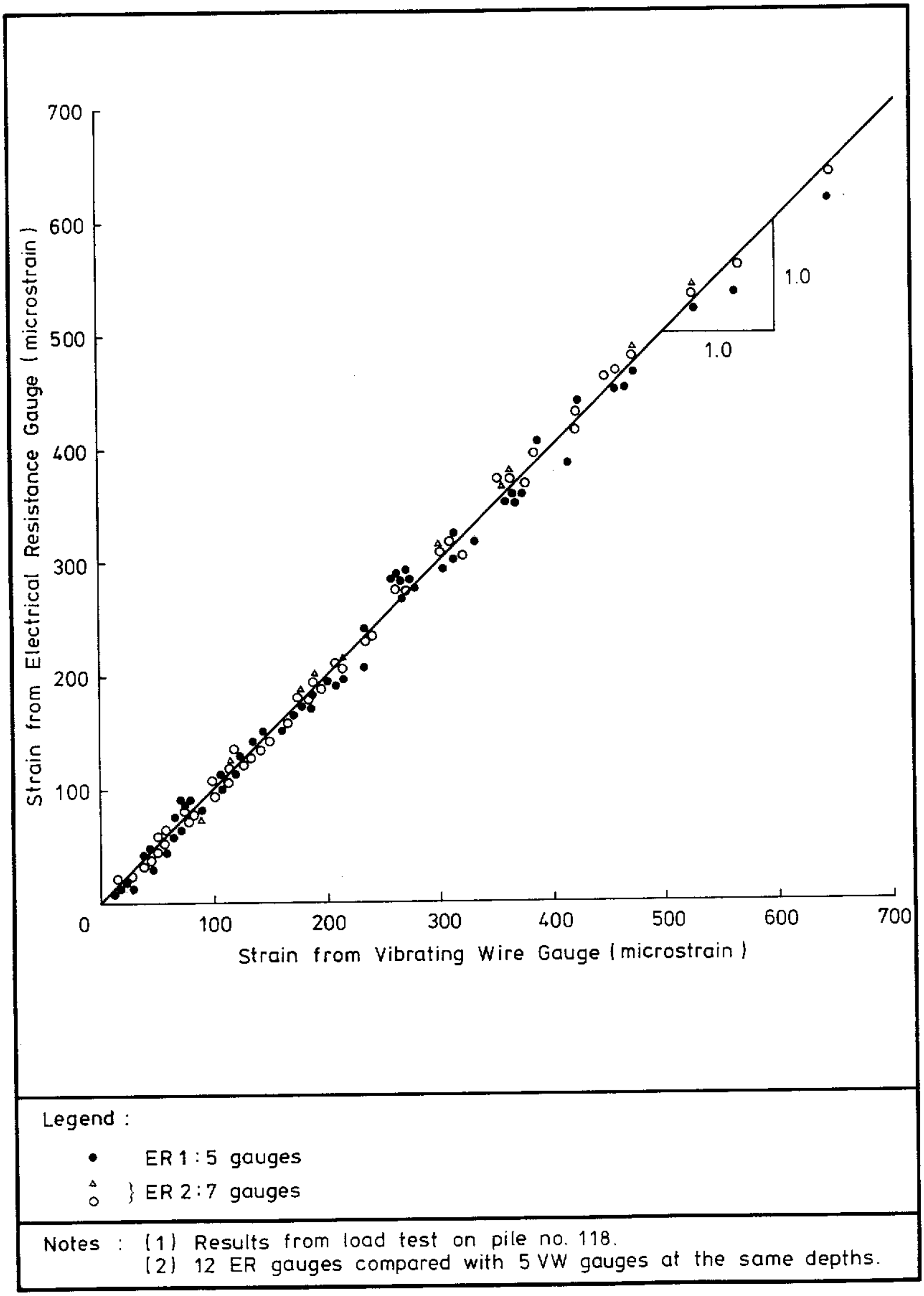

Figure 8 - Comparison of Strains Calculated from VW Strain Gauge and ER Strain Gauge Readings (See Appendix B)

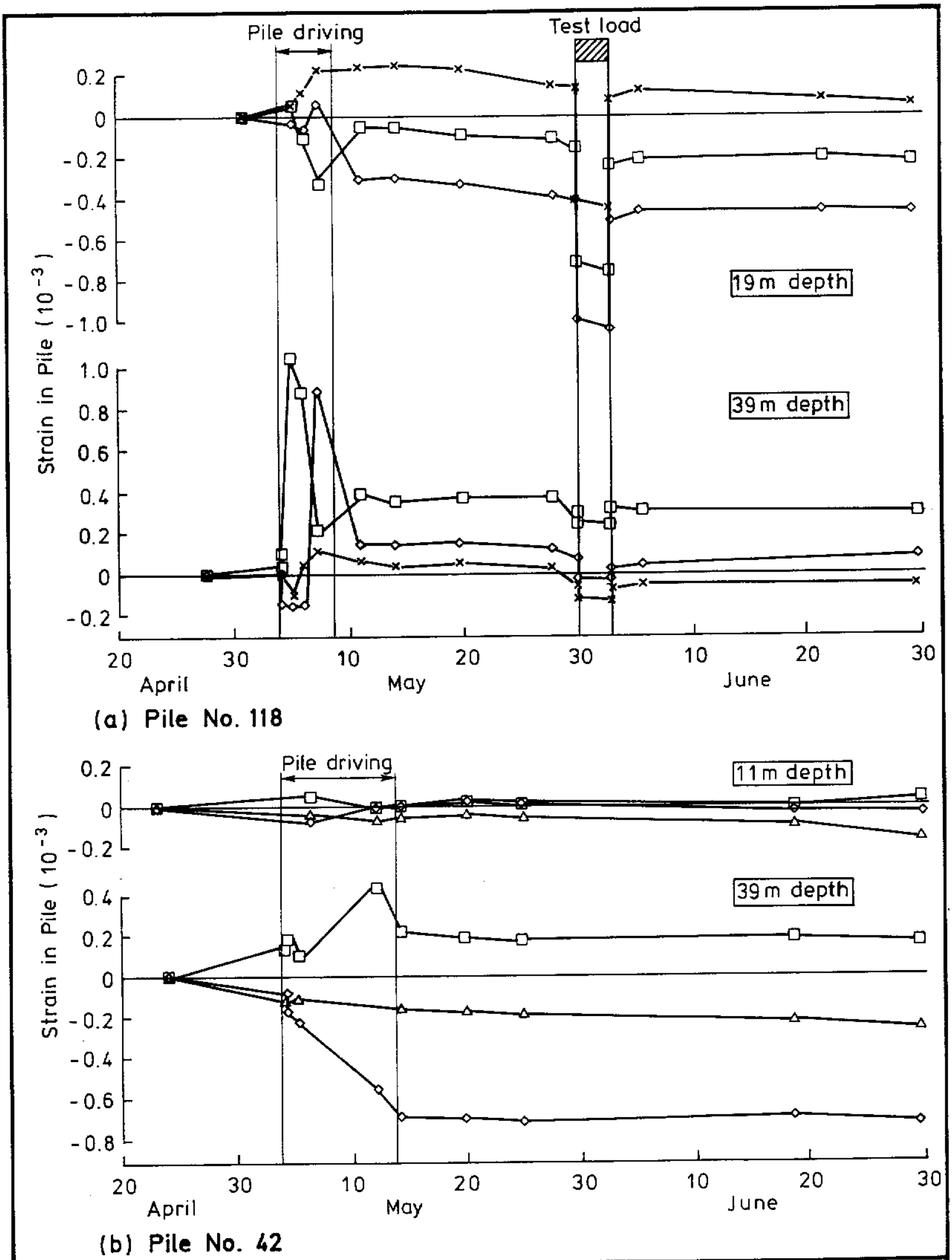

Note : Strains were measured after driving of each pile section during the driving stage.

Figure 9 - Results from Strain Monitoring at Three Positions in Piles Nos. 118 & 42 over a Two Month Period

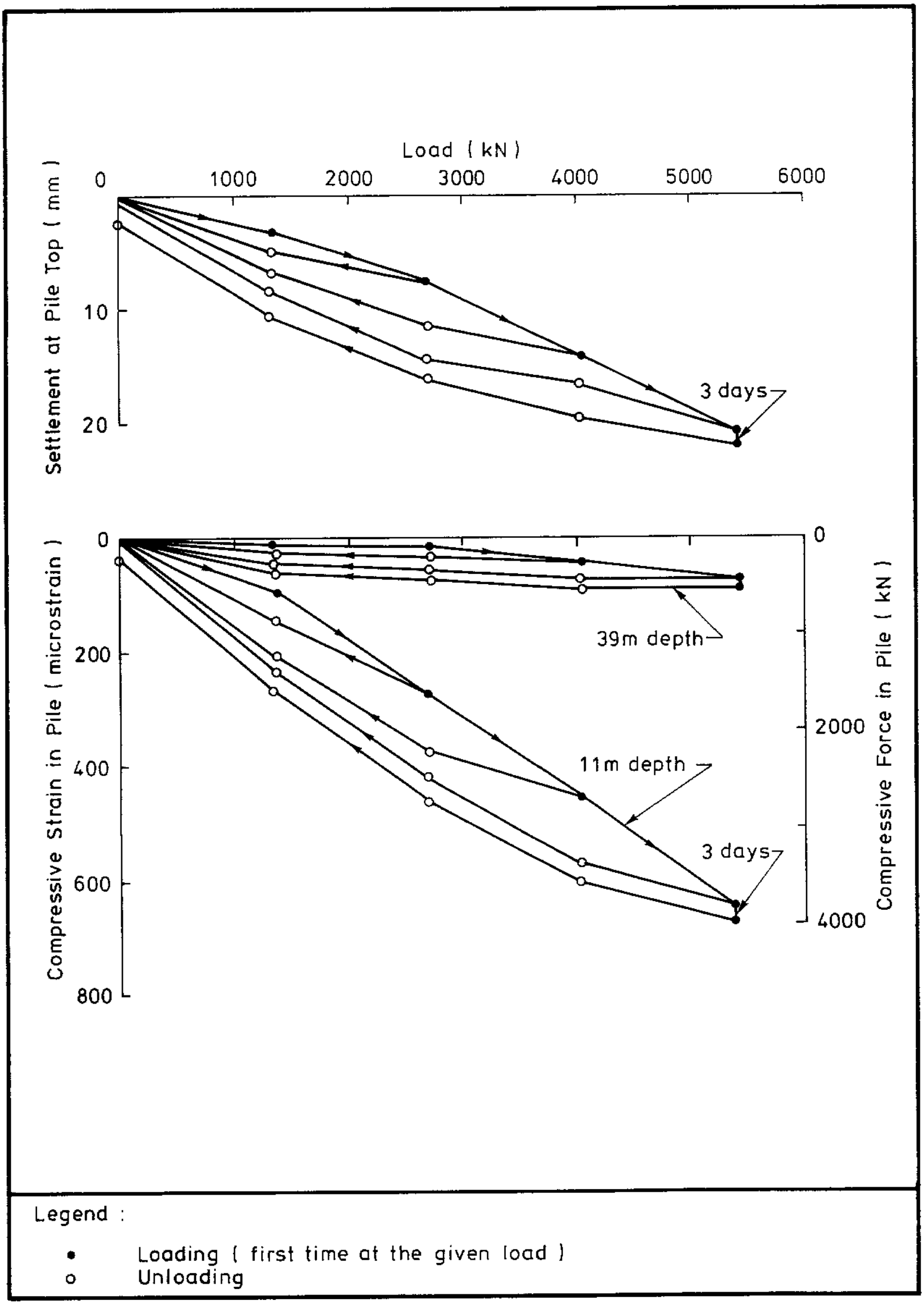

Figure 10 - Load/Settlement and Load/Strain Force Relationships Obtained from Load Test on Pile No. 118

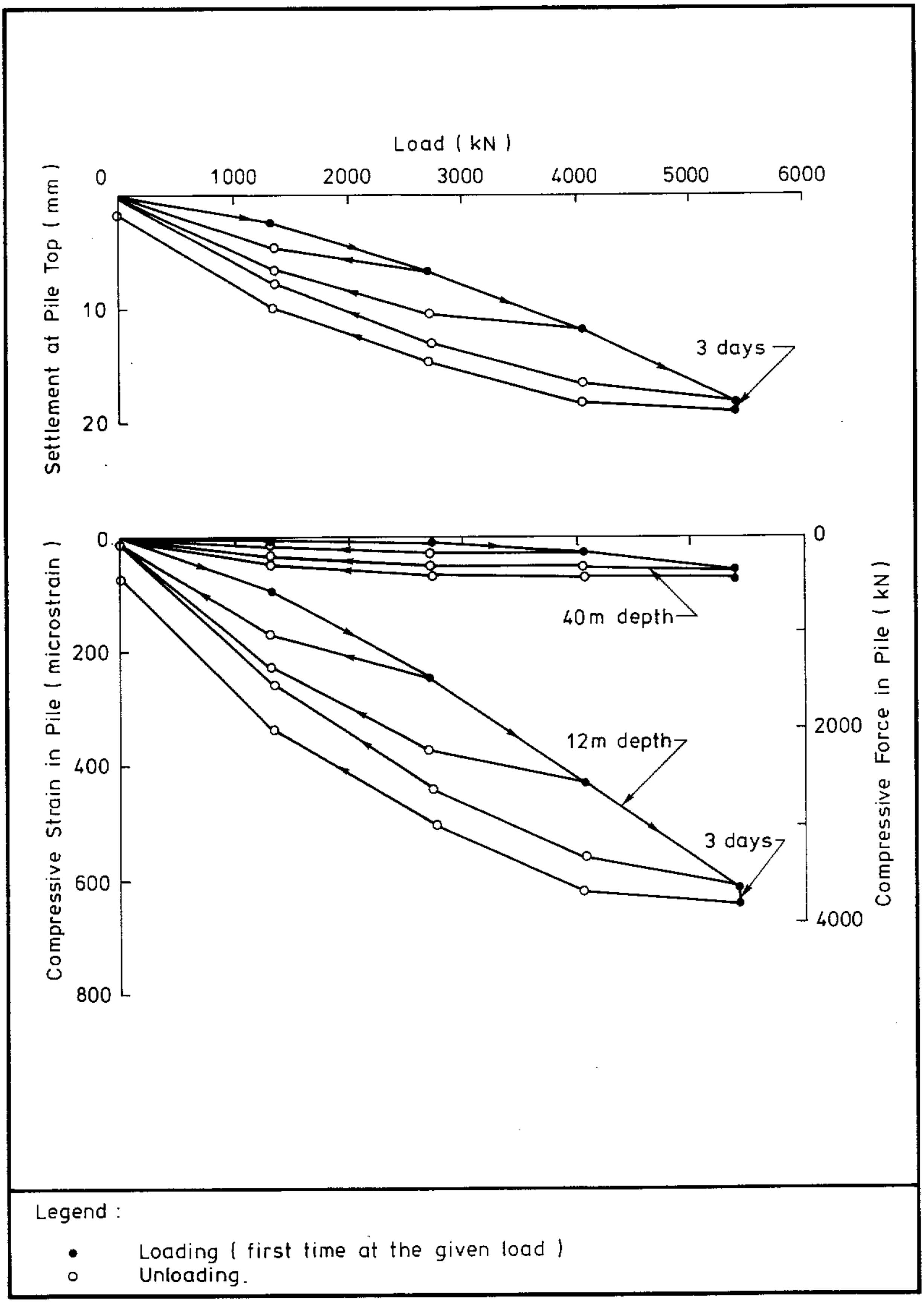

Figure 11 - Load/Settlement and Load/Strain Force Relationships Obtained from Load Test on Pile No. 58

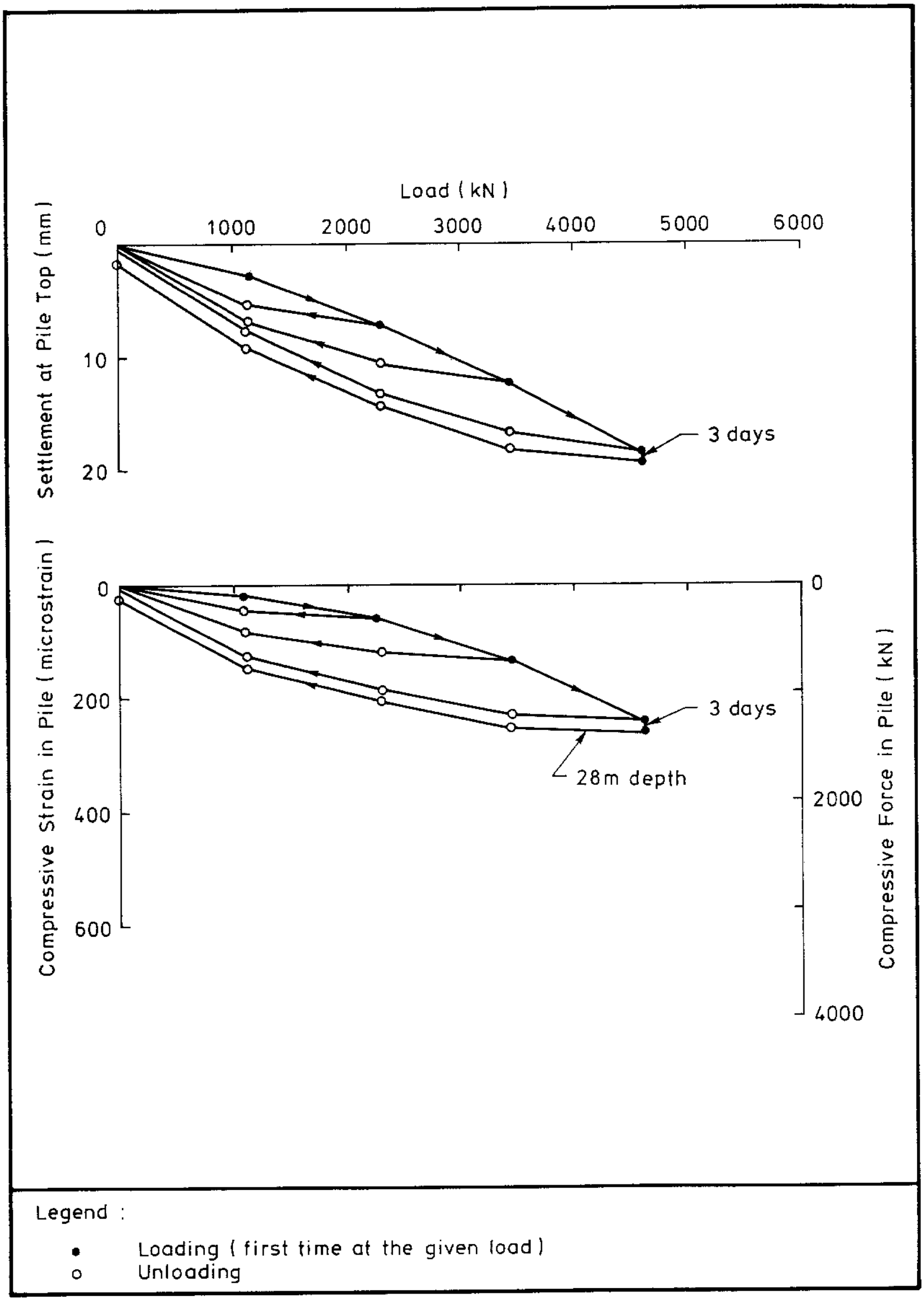

Figure 12 - Load/Settlement and Load/Strain Force Relationships Obtained from Load Test on Pile No. 26A

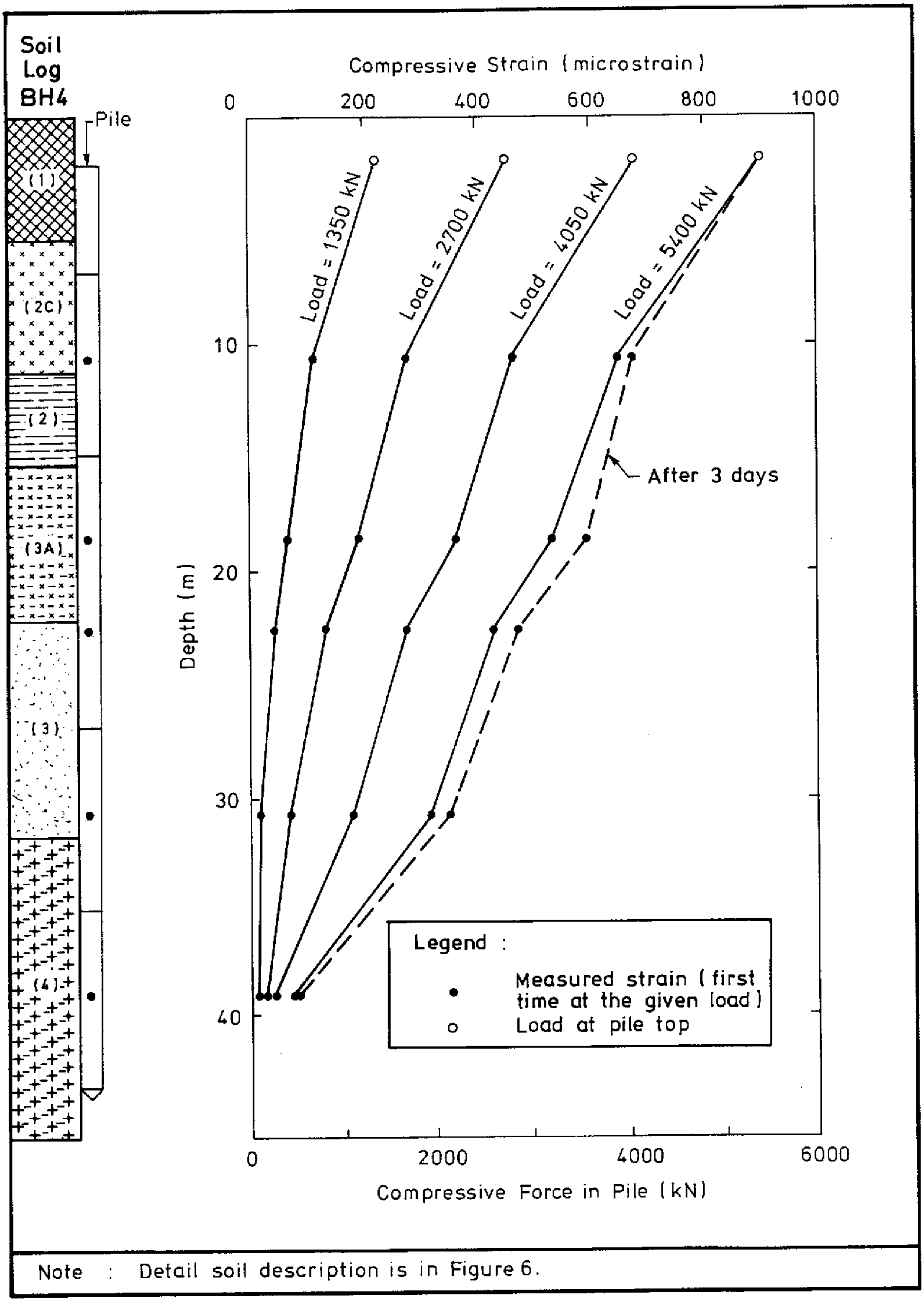

Figure 13 - Distribution of Compressive Strain and Force in Pile No. 118 during Pile Load Test

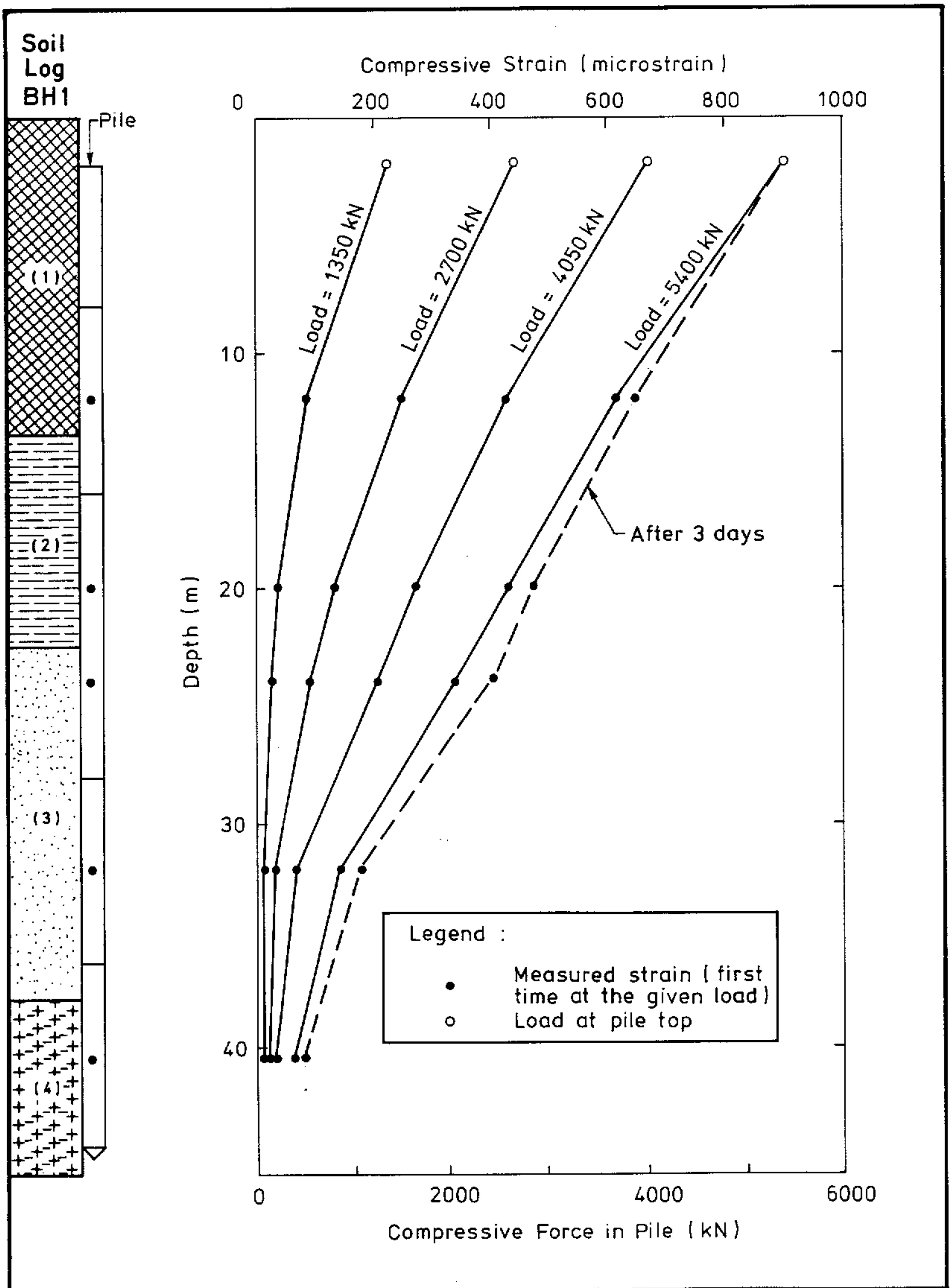

Note : Detail soil description is in Figure 6.

Figure 14 - Distribution of Compressive Strain and Force in Pile No. 58 during Pile Load Test

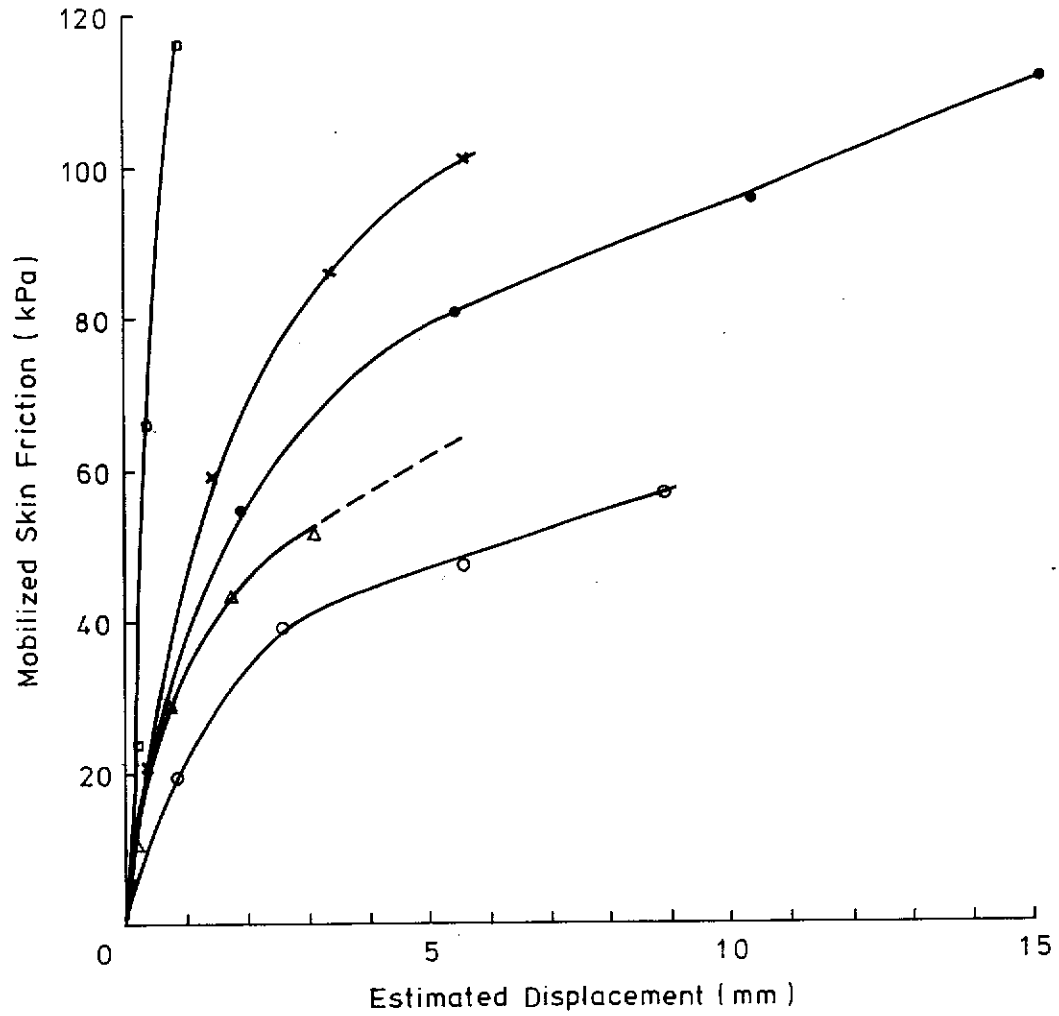

Legend :

	Depth (m)	Soil Type
●	2 - 11	FILL (1) / SILT (2C)
○	11 - 19	CLAY (2) / (3A)
×	19 - 23	CLAY (3A) / SAND (3)
△	23 - 31	SAND (3)
□	31 - 39	WEATHERED GRANITE (4)

Notes : (1) Soil descriptions are given in Figure 6.
(2) Gauge positions relative to soil strata are shown in Figure 13.

Figure 15 - Relationship between Mobilized Skin Friction on Piles and the Estimated Soil/Pile Displacement for Pile No. 118

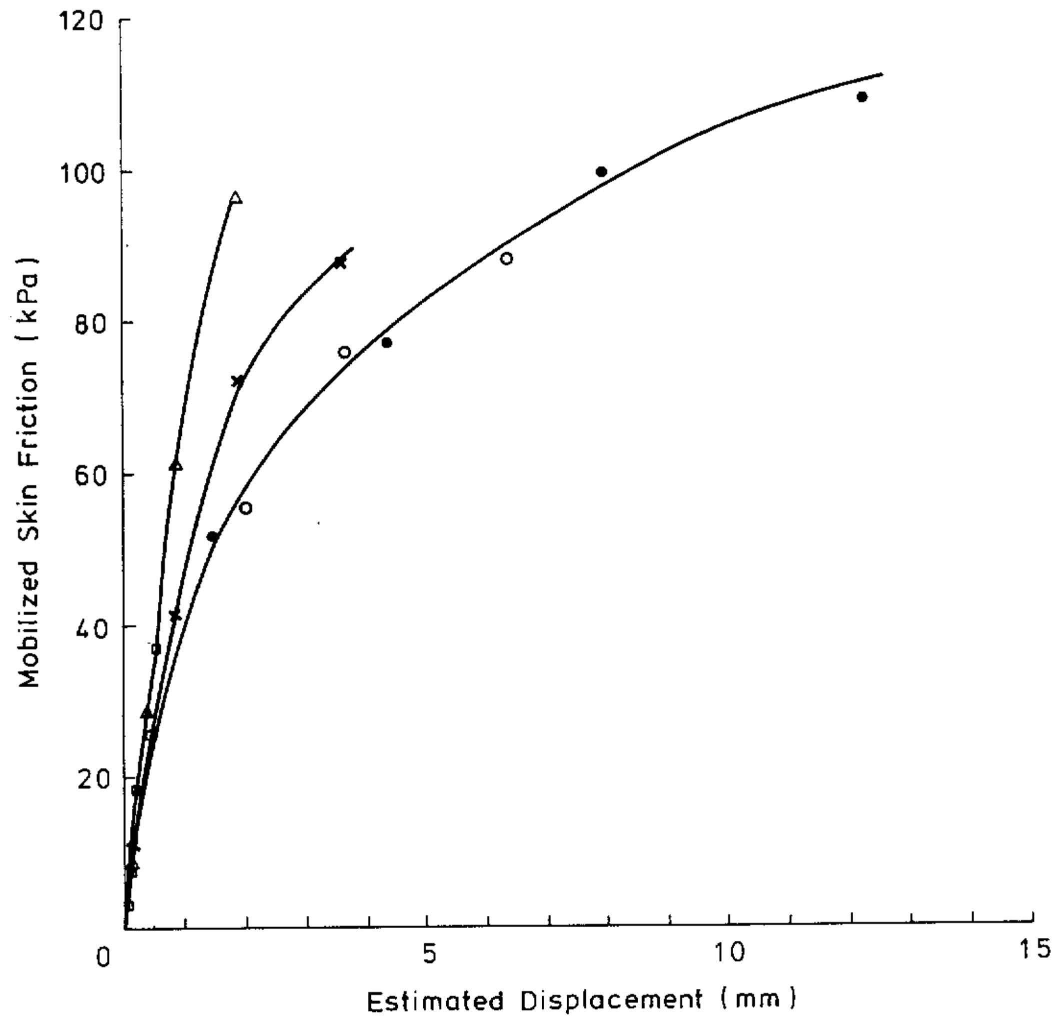

Legend :	Depth (m)	Soil Type
•	2 - 12	FILL (1)
o	12 - 20	CLAY (2)
×	20 - 24	SAND (3) / CLAY (2)
Δ	24 - 32	SAND (3)
□	32 - 40	SAND (3) / WEATHERED GRANITE (4)

Notes : (1) Soil descriptions are given in Figure 6.
(2) Gauge positions relative to soil strata are shown in Figure 14.

Figure 16 - Relationship between Mobilized Skin Friction on Piles and the Estimated Soil/Pile Displacement for Pile No. 58

LIST OF PLATES

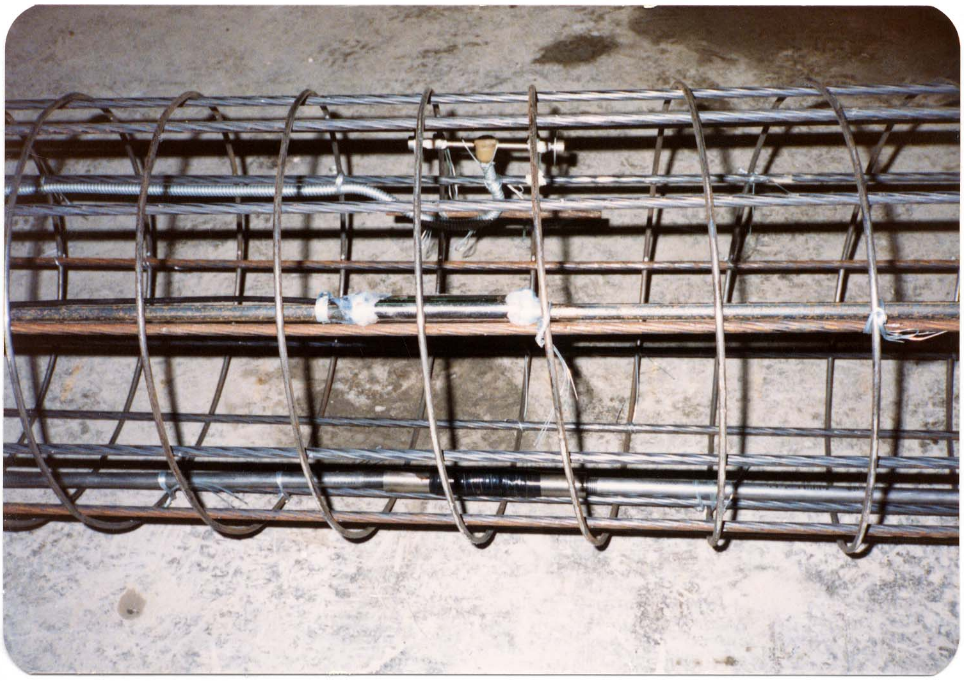

Negative No. SP 8702819 Date : 8.4.87

Plate 1 - Strain Gauges Attached to Reinforcement

Negative No. SP 8702016 Date : 10.3.87

Plate 2 - Concrete Poured into the Pile Mould

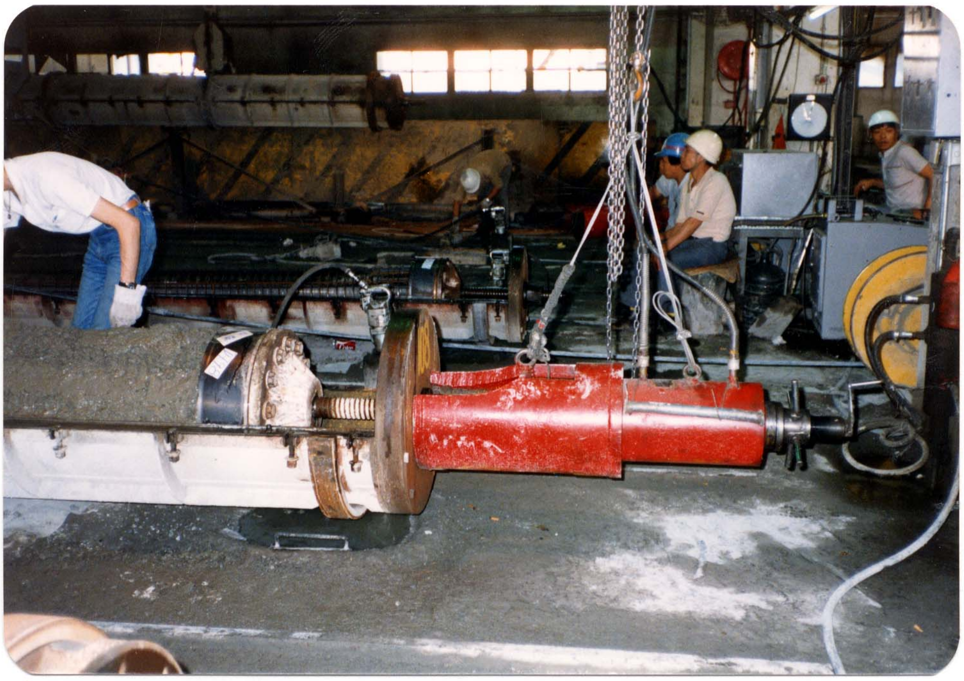

Negative No. SP 8702823 Date : 8.4.87

Plate 3 - Prestressing the Reinforcement

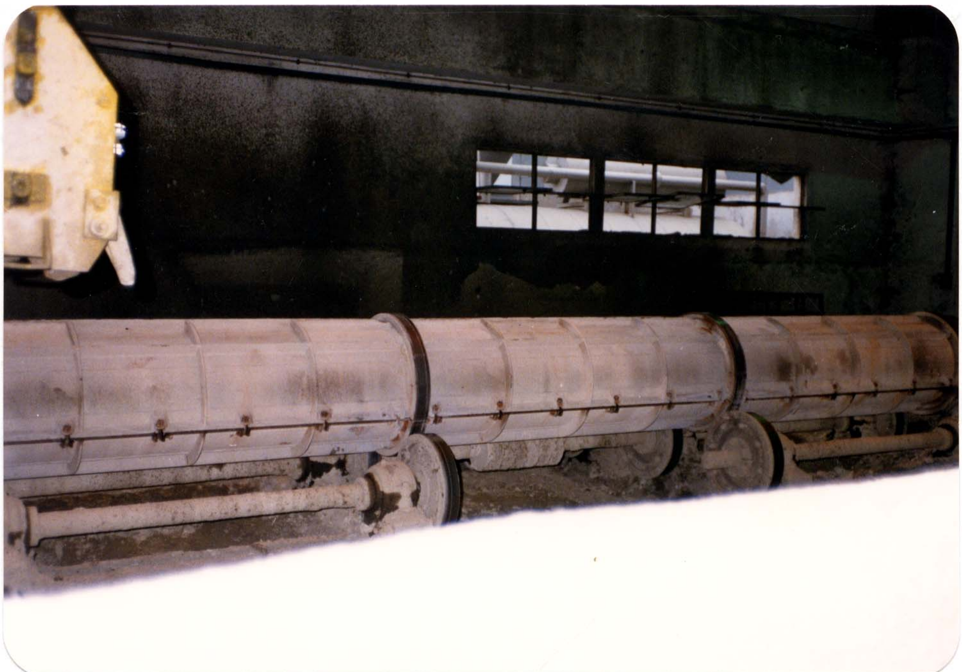

Negative No. SP 8702020 Date : 10.3.87

Plate 4 - Spinning the Mould

Negative No. SP 8702509 Date : 26.3.87

Plate 5 - Steam Curing of Pile Sections in Autoclave

Negative No. SP 8702401 Date : 13.3.87

Plate 6 - Bending Test of a Pile Section

Negative No. SP 8702724A Date : 30.3.87

Plate 7 - Driving an Instrumented Pile

Negative No. SP 87036A01 Date : 12.5.87

Plate 8 - Handing the Strain Gauge Cables

Negative No. SP 8702721 Date : 30.3.87

Plate 9 - Weld Connection of Pile Sections

Negative No. SP 87036A11 Date : 12.5.87

Plate 10 - Measurement for Final Set

Negative No. SP 8703903   Date : 12.6.87

Plate 11 - Kentledge for Pile Load Test

Negative No. SP 8703911   Date : 30.5.87

Plate 12 - Load Test Set-up

Negative No. SP 8703906   Date : 12.6.87

Plate 13 - Terminal Boxes for Cables at the End of Piling Work

APPENDIX A

DETERMINATION OF MODULUS OF ELASTICITY OF PILES

APPENDIX A : DETERMINATION OF MODULUS OF ELASTICITY OF PILES

A bending test on an instrumented pile section (later incorporated into pile no. 26A) was carried out in the pile testing area of the Daido Concrete Ltd. plant at Tai Po. The test set-up was as shown in Figure A-1. The pile section was 8 m in length, and this was placed on two supports, one at 1.6 m from each end of the section. The load was applied using a hydraulic jack at two points, 0.5 m either side of the section mid-point. With this arrangement there were no shear forces in the middle 1.0 m length of the pile. The total load was read from a gauge attached to the jack, and the deflection at mid-point of the pile section was measured by means of a dial gauge.

From the measured load and deflection, the modulus of elasticity of the hollow pile section was calculated from (Granet, 1980) :

$$E = \frac{Pa}{48Iz}(3L^2 - 4a^2)$$

Where P = total load

z = deflection at mid-point

From Figure A.1, $P/z = 4.94 \times 10^4$ kN/m

a = distance between a support and a load point = 1.9 m

L = distance between supports = 4.8 m

I = second moment of area of the pile = $\frac{\pi}{4}(R_1^4 - R_2^4)$

R_1 = outside radius = 0.25 m

R_2 = inside radius (measured) = 0.14 m

$I = 2.766 \times 10^{-3}$ m^4

Therefore E = 38.6 GPa.

This value is within 2.5% of the value of 37.7 GPa quoted by Daido Concrete Ltd.

The hollows of the instrumented piles were filled with concrete grout after being driven to final depth. Three concrete grout cylinder samples were obtained during the grouting on 14 May, and they were tested in the Public Works Central Laboratory at North Point after 28 days. Four sets of the results are shown in Figure A.2. The average modulus of elasticity is 11.5 GPa.

The combined compressibility of the pile section and concrete grout was then calculated, using the nominal outside diameter of 500 mm, and wall thicknesses of 125 mm and 100 mm for the thick and thin pile sections respectively. From the relation :

$$F = AEs = (A_1E_1 + A_2E_2)s$$

Where F = pile axial force

A_1, A_2 = cross sectional areas of concrete and hollow in the hollow pile

E_1, E_2 = moduli of elasticity of hollow pile and concrete grout

s = axial strain, being equal across the section

For 125 mm thick pile, 1 microstrain represents about 6 kN axial force.
For 100 mm thick pile, 1 microstrain represents about 5.2 kN axial force.

The conversion of strain to axial force is not sensitive to modulus of elasticity of the grout. If E of grout is in error by 50%, the conversion will be in error by only 3.5% for the thicker walled pile.

LIST OF FIGURES

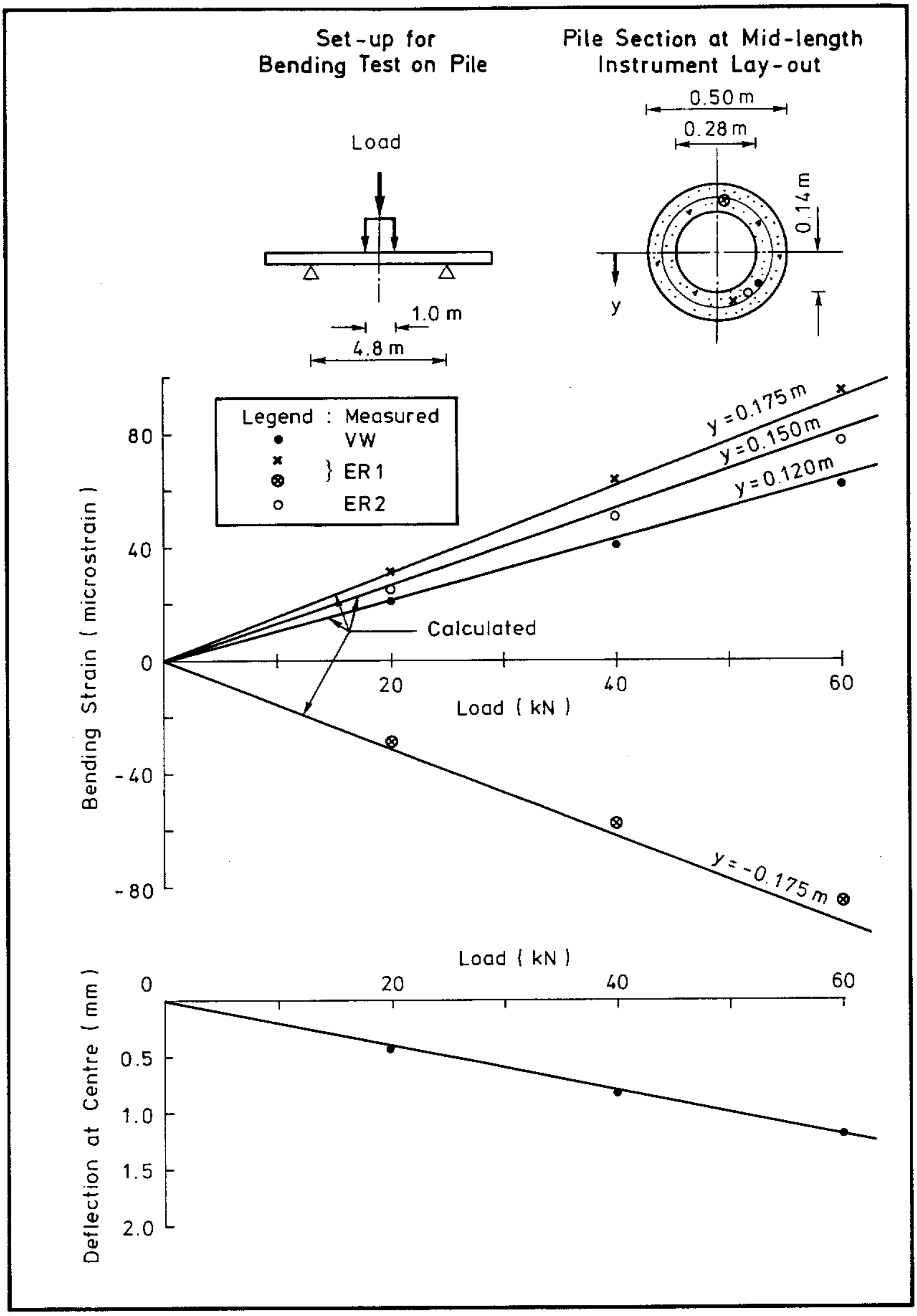

Figure A1 - Results from Bending Test on Pile Section

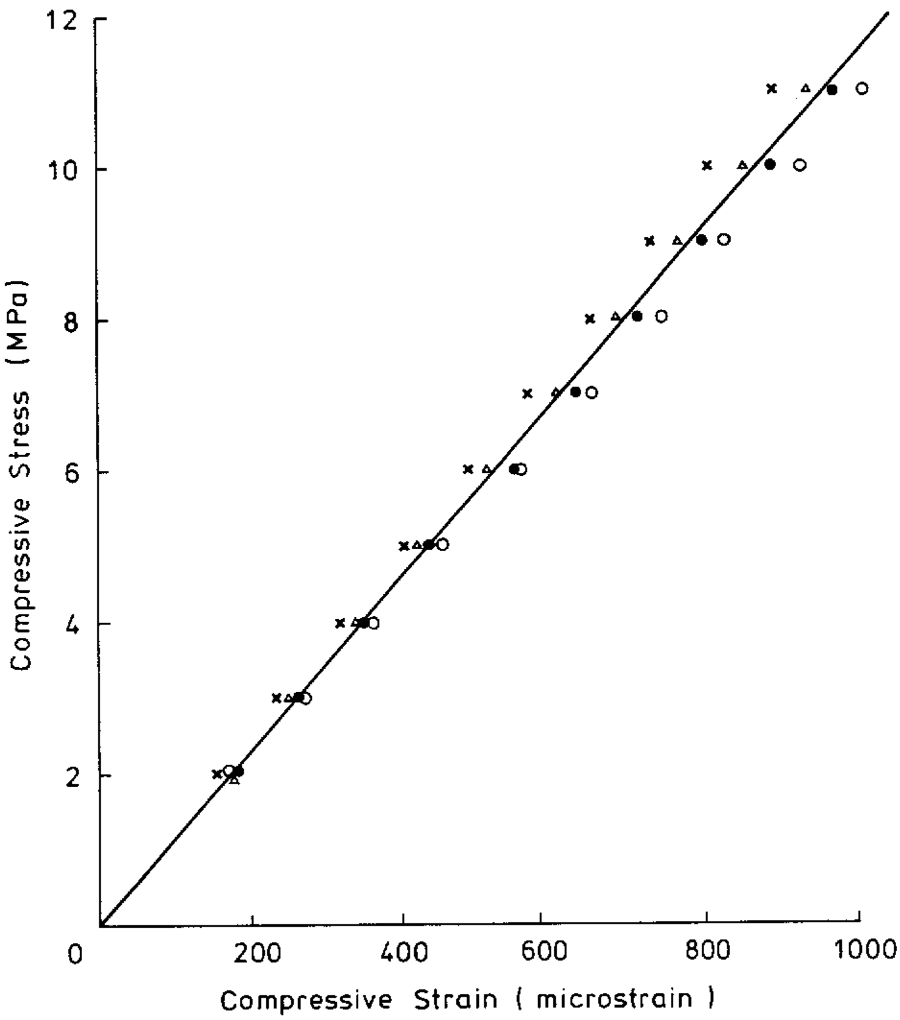

Figure A2 - Stress/Strain Relationship Obtained from Compression Tests on Cylinder Samples of Concrete Grout Used to Fill Pile Hollow

APPENDIX B

VERIFICATION OF STRAIN GAUGE READINGS

APPENDIX B : VERIFICATION OF STRAIN GAUGE READINGS

Strain gauge manufacturers usually provide a 'gauge factor' for calculation of strains from gauge readings, on the basis of a test on a specimen from a large batch of gauges. This may be used for calculation as a first approximation. Inevitably, however, there are variability within the batch and differences between conditions during calibration and use in the field. It is prudent, therefore, to examine the gauge responses under working conditions.

The bending test described in Appendix A allowed assessment of strain gauge performance. The results from the strain measurement during the bending test are shown in Figure A.1. The gauges at the top and bottom of the section showed compressive and tensile strains respectively. The gauge readings were in good agreement with the calculated strains, which were obtained from :

$$s = \frac{Pay}{2EI}$$

where y = vertical distance from bending neutral axis (in m)

Other symbols are the same as those in Appendix A.

Therefore : $s = 8.9\,Py$ microstrains

The test enabled assessment of the gauges after embedment in the pile section. It is noted, however, that the positions of the gauges with respect to the neutral axis cannot be determined precisely. Therefore the test confirmed correct readings of gauges to within about 5% (ER1 readings in Figure A.1 have been adjusted, see below).

The load test provided direct test of a large number of gauges at the same time. In pile no. 118, there were five VW gauges, five ER1 gauges and nine ER2 gauges placed at five depths along the pile (Section 3.3.1, Figure 7). Independent checks can be made because VW gauges operate entirely differently from ER gauges (see operating principles in Hanna, 1973 and 1985). The direct readings obtained from ER1 and ER2 gauges were compared with those obtained from VW gauges at the same depths. The relevant plot is shown in Figure B.1. Seven of the ER2 gauges provided almost identical readings to those obtained from VW gauges. All five of the ER1 gauges provided consistently slightly higher readings, by a factor of about 1.2, when compared with five VW gauges and seven ER2 gauges. The remaining two ER2 gauges gave anomalous readings compared to all other gauges.

It was clear that five VW and seven ER2 gauges provided consistent readings. Since the orientation of each section was random, the consistent slight deviation of all five ER1 gauges cannot be due to bending or other external causes. Therefore, a factor of 1.2 was applied to all ER1 gauge readings. Two ER2 gauges provided non-linear responses, and the readings must be discarded. This could have been due to slight damage (possibly buckling) during casting and driving. They demonstrated that each reading must be carefully checked to determine whether it is reasonable, before it is used in the analysis. The correlation after these adjustments is shown in Figure 8.

The agreement between strains obtained from ER gauges and VW gauges, with deviations of less than 5%, confirmed definitely the validity of the measurements. The close agreement between gauges at the same depths also confirmed that there was negligible bending when a static load was applied. This is in contrast to the large bending strains generated during pile driving.

This comparison exercise provided many advantages over the laboratory calibration of individual gauges, which is time consuming and may not represent the response of gauges embedded in a pile. A limited number of laboratory calibration tests were carried out in this study and provided similar results to those discussed above. However, the load test results were considered more representative because they involved a large number of gauges tested at the same time under the same load.

LIST OF FIGURES

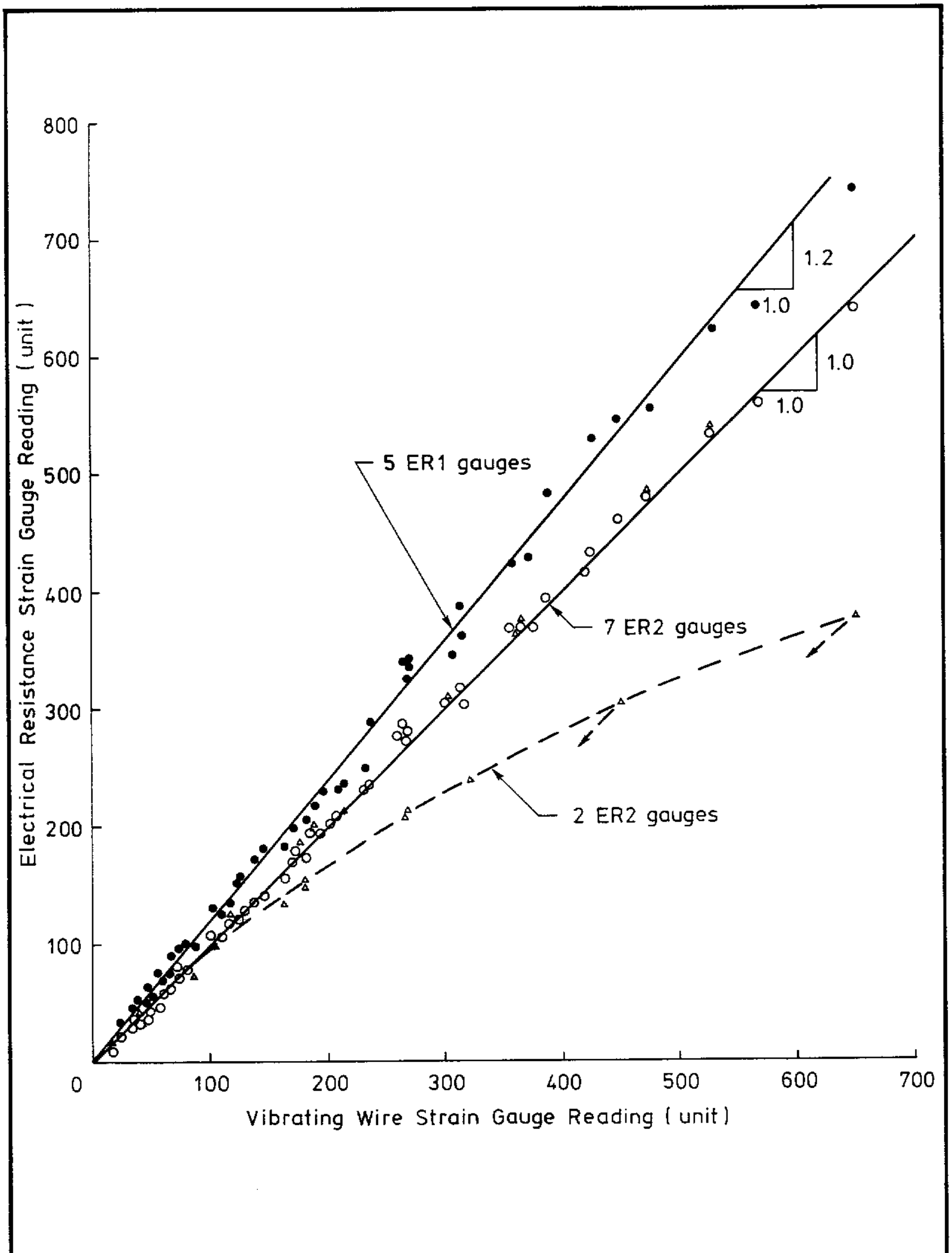

Notes : (1) Results from load test on pile no. 118.
(2) 14 ER gauges compared with 5 VW gauges at the same depths.

Figure B1 - Comparison of Readings Obtained from VW Strain Gauges and ER Strain Gauges

APPENDIX C

RELEVANT MATHEMATICAL EXPRESSIONS

CONTENTS

C.1 Estimation of Bending Strains and Bending Moments

The axial force is related to axial strain as follows :

$$F = AEs = (A_1E_1 + A_2E_2)s$$

The parameters are defined in Appendix A.

Strain gauge readings are obtained at three gauge positions. The positions are approximately equally spaced 120° apart on a circle of radius y. The measured strains, in clockwise sequence from north as viewed from top down, are r_1, r_2 and r_3.

The average of the three strains is the axial strain, s :

$$s = \frac{1}{3}(r_1 + r_2 + r_3)$$

The difference between each of these strains and the axial strain is the bending strain :

$$e_1 = r_1 - s = e \cos(t_1 - x)$$

$$e_2 = r_2 - s = e \cos(t_2 - x)$$

$$e_3 = r_3 - s = e \cos(t_3 - x)$$

where e is the maximum bending strain (positive and negative values on opposite sides across the pile diameter) within the circle of radius y; t_1, t_2 and t_3 are the angles of respective gauge positions measured clockwise from north, and x is the angle to the position of the maximum bending strain measured clockwise from north. e is zero in the case of no bending.

e and x are unknowns and can be found from :

$$t_1 - x = \tan^{-1}\left[\frac{e_3 - e_2}{\sqrt{3}\,e_1}\right]$$

$$e = \frac{e_1}{\cos(t_1 - x)}$$

This calculation allows $(t_1 - x)$ to be within $\pm 90°$ and e could take positive or negative value.

The bending moment can be estimated from :

$$M = \left(\frac{e}{y}\right)EI$$

For combined pile and grout section :

$$M = \left(\frac{e}{y}\right)(E_1I_1 + E_1I_2)$$

I_1 I_2 - second moment of area of the hollow pile and of the concrete grout in the hollow.

In the case where the three gauge positions are far from being equally spaced, the average of the three strains will not be equal to axial strain. Solutions for s, e and x may be found by other methods such as Newton-Ralphson. This involves formation of a Jacobian matrix from the above three equations for e_1, e_2 and e_3, and solving the matrix equation by iteration.

C.2 Formulae for Skin Friction

Skin friction is developed when there is relative displacement between the pile and the surrounding soil. It reaches a maximum value and remains almost constant when the displacement exceeds a certain limit. The limit to full mobilization of friction is in the order of a few millimetres (Broms, 1979). The negative skin friction will, in general, be less than the positive skin friction. The limit skin friction may be expressed by the α-method as a function of insitu undrained shear strength of the soil, as follows :

$$f = \alpha s_u$$

where f = skin friction
α = empirical constant determined from test results
s_u = undrained shear strength of soil

In effective stress analysis, the skin friction is related to the vertical effective stress in the ground (the β-method) as follows :

$$f = \sigma_v' \, K \tan \phi_a' = \beta \sigma_v'$$

where σ_v' = effective overburden pressure (vertical) in soil
K = coefficient of lateral earth pressure
ϕ'_a = effective friction angle of soil with respect to the pile surface
β = equal to ($K \tan \phi'_a$), which can be determined empirically from field tests on piles

In another approach reviewed by Tomlinson (1977) and Karlsrud & Haugen (1985) the friction is related to both the effective overburden pressure and the undrained shear strength of soil, the τ-method, as follows :

$$f = \tau \, (\sigma_v' + 2s_u)$$

τ = empirical constant determined from test results.

The α- and β-methods are both commonly used. For the soil strata typically encountered in reclamation areas in Hong Kong, the β-method is considered to be more suitable.

C.3 Calculation of Strains from Instrument Readings

For electrical resistance (ER) strain gauges, the readings obtained from the read-out unit are approximately in units of microstrain. The difference between two readings is the change in strain during the elapsed time. This should be modified by an appropriate gauge factor (multiplied by 2.0/gauge factor, which is approximately 1.0). Increases in the readings indicate extension and decreases indicate compression. For ER2 gauges, the verification in Appendix B showed that the strain may be found, with adequate accuracy, directly from :

$$s = (R - R_o)$$

where s = strain in microstrain units (change in length of one part per million)
R = reading at a particular time
R_o = initial reading, i.e. the assumed zero strain level

Each instrument consisted of two gauges attached to a steel rod. The strain is therefore the average of the strains obtained from the two gauges.

For ER1, an adjustment factor of 1.2 is required (verification is given in Appendix B) :

$$s = \frac{1}{1.2}(R - R_0)$$

For vibrating wire (VW) strain gauges, the reading is units of time rather than strain. The display shows the time taken for the wire to vibrate one hundred cycles, in units of 10^{-5} seconds (ten microseconds). The normal range of the frequency is about 950 Hertz, corresponding to a reading of around 10000. For the gauges used in this study, TES/5.5, the strain can be calculated from

$$s = 3.0 \times 10^{11}\left(\frac{1}{T^2} - \frac{1}{T_0^2}\right)$$

where T = reading at a particular time
T_o = initial reading, i.e. the assumed zero strain level